lubricants

MDPI

Review

A Review of Mesoscopic Damage and Its Discrete Performance in Local Functional Grooves of Cageless Ball Bearings

Enwen Zhou [1,2,3], Yibo Wang [1], Jingwei Zhang [1,2,3] and Yuan Zhang [2,*]

[1] Railway Locomotive and Rolling Stock Faculty, Jilin Tiedao University, Jilin 132299, China; zhouenwen@jt-edu.com.cn (E.Z.); wangyibo@jt-edu.com.cn (Y.W.); zhangjingwei@jt-edu.com.cn (J.Z.)
[2] Key Laboratory of Advanced Manufacturing and Intelligent Technology, Ministry of Education, Harbin University of Science and Technology, Harbin 150080, China
[3] Goertek Inc. Postdoctoral Research Station, Goertek Co., Ltd., Weifang 261031, China
* Correspondence: irhpa01861@126.com

Abstract

Cageless ball bearings, due to their larger number of rolling elements and stronger load-bearing capacity, are widely used in active magnetic bearing systems, serving as protective bearings. However, due to the lack of traditional cages to isolate adjacent rolling elements in cageless ball bearings, cumulative collisions are inevitable, leading to severe friction and heating. Although scholars have proposed using cageless ball bearings with local functional grooves as protective bearings for magnetic bearings, and conducted relevant theoretical and experimental research on them, the impact of bearing wear with local functional grooves on the dispersion effect remains to be studied. Wear of local functional grooves can cause their edges to expand outward, altering the contact radius between the rolling elements and the grooves. This change also affects the orbital velocity of the rolling elements passing through the grooves, leading to collisions between adjacent rolling elements. In severe cases, this can result in the rolling elements failing due to self-dispersion. By studying the impact of the degree of damage to local functional grooves on the self-dispersion behavior of rolling elements, we can assess the lifespan of protective bearings, facilitating timely replacement and reducing major accidents and economic losses caused by bearing failure.

Keywords: cageless ball bearing; local functional groove; non-smooth behavior; mesoscale damage; discrete performance

1. Introduction

Rolling bearings are indispensable core fundamental components of rotating machinery, widely used in key fields such as high-speed rail transit, aerospace, large-scale wind power, precision machine tools, and intelligent manufacturing equipment. Their service reliability directly determines the operational stability and service life of the entire machine system. Due to advantages such as low friction, low power consumption, high efficiency, and ease of maintenance [1,2], rolling bearings have become one of the most widely applied supporting elements in modern industrial systems.

With the rapid development of high-end equipment towards high speed, high precision, heavy load, and intelligence, the operational reliability of bearings under complex and extreme working conditions faces severe challenges. Although a complete industrial system for bearing manufacturing has been established globally, there remain core technological bottlenecks in the field of high-precision, high-reliability bearings [3,4]. Key product

Check for updates

Received: 20 September 2026
Revised: 4 October 2026
Accepted: 14 October 2026
Published: 15 October 2026

Copyright: © 2026 by the authors. Licensee MDPI, Basel, Switzerland. This article is an open access article distributed under the terms and conditions of the Creative Commons Attribution (CC BY) license.

performance and stability are insufficient, restricting the improvement of autonomous controllability of high-end equipment. Therefore, revealing the failure evolution mechanisms of bearings and enhancing operational reliability under extreme conditions have become common technical challenges urgently to be addressed in the high-end equipment sector.

Bearing failure is the primary cause of rotating machinery faults and major safety accidents. Statistical data show that about 44% of large asynchronous motor failures [5] and 30% of rotating machinery downtime incidents [6] are caused by bearing failure. Inner and outer raceway damages account for more than 90% of bearing failures, with typical forms including surface spalling, creep, wear, and pseudo-Brinell indentations [7]. Historically, multiple catastrophic events such as train derailments and power generation equipment damage have been directly linked to sudden bearing failures, highlighting the urgency and importance of researching bearing failure mechanisms and improving operational reliability. Apart from external factors like poor lubrication and improper assembly, the dynamic instability of rolling elements is a key intrinsic factor inducing contact impact and early damage to raceways [8]. Nonlinear changes in rolling element motion posture exacerbate the non-smooth behavior at the contact interface, complicating the bearing system's dynamic behavior, thereby accelerating damage evolution and reducing service life [9].

Magnetic bearings, as a type of non-contact precision support component, have outstanding advantages such as no mechanical wear, low vibration, adaptability to high speeds, and high stability. They have rapidly developed and been scaled in high-end fields such as aero-engine main shafts, high-speed grinding spindles, energy storage flywheels, and semiconductor equipment [10,11]. However, when magnetic bearings lose power or fail, the backup bearing must instantly withstand the impact from the high-speed rotor and provide temporary support, forming a critical weak link in ensuring system safety. Traditional rolling bearings with cages have insufficient impact resistance and tend to seize under high-speed conditions [12,13]. Cageless ball bearings, although possessing higher load capacity, suffer significantly from collision friction among rolling elements, leading to excessive temperature rise and early failure [14,15].

To suppress contact collisions among rolling elements in cageless ball bearings, researchers have proposed innovative designs introducing local functional grooves in the raceways. By controlling the differential orbital velocities of rolling elements, this achieves self-dispersing effects, effectively reducing contact impact and temperature rise [16]. Related studies have established instantaneous motion models of rolling elements, collision-friction dynamic models, and contact stress analysis methods, clarifying the influence laws of groove geometric parameters on self-dispersing effects and providing theoretical support for optimizing protective bearing performance [17]. However, the influence mechanism of wear evolution of local functional grooves on rolling element self-dispersing behavior and long-term bearing reliability has not yet been systematically elucidated. The coupling relationship between contact characteristics and dynamic response during the wear process still lacks in-depth understanding, restricting further development in protective bearing life prediction and full lifecycle optimized design.

This paper systematically reviews the current research status of rolling bearing non-smooth contact response, damage evolution mechanisms, and microscopic characterization methods; analyzes the core progress in structural design, dynamic modeling, and performance evaluation of cageless ball bearings with local functional grooves; clarifies the limitations and deficiencies of current research in multi-posture contact coupling, three-dimensional damage evolution, and microscopic force chain transmission; and prospects future research directions integrating multi-scale modeling, digital simulation, and experimental validation. The aim is to provide theoretical references and technical support

for improving the reliability of high-end rolling bearings and the full lifecycle optimized design of protective bearings.

For the sake of clarity, the remainder of this review is organized as follows. Sections 2–4 provide an overview of the state of the art, namely the non-smooth contact response of rolling bearings, the research methods for bearing damage, and the mesoscopic damage characterization methods. Section 5 provides a critical discussion of the reviewed work, in which the concept of the non-smooth surface and the influence of the lubricant and of its water content are clarified, the reviewed models are compared, and the limitations of the existing studies are identified. Section 6 is devoted exclusively to the authors' proposal for future and ongoing research, which is therefore clearly separated from the overview. Section 7 summarizes the main conclusions of the review.

2. Research on the Non-Smooth Contact Response of Rolling Bearings

As the primary components of rolling bearings, rolling elements play a decisive role in determining the overall kinematic and mechanical performance of the bearing during operation. Due to the cyclic and alternating stresses between the rolling elements and the raceways, prolonged contact makes them the components most prone to fatigue failure in rolling bearings [18,19]. At high rotational speeds, rolling bearings are highly prone to violent gyroscopic motion, which generates significant internal friction and causes severe damage [20]. When the rolling elements come into contact with the raceways, the resulting contact angle exerts a certain influence on the rolling elements' spin and rotation, leading to slippage phenomena [21]. Therefore, clarifying the motion laws of rolling elements and analyzing their non-smooth behavior under different motion states not only aids theoretical modeling research on rolling bearings but also holds extreme significance for engineering issues such as bearing wear, failure, and service life.

2.1. Modeling of Non-Smooth Contact in Rolling Elements

In the 1960s, Jones [22] proposed a raceway-controlled method, assuming that rolling elements move on the raceway via pure rolling without any other motions such as spin or rotation. He employed a quasi-static approach to establish a system of mechanical equilibrium equations between the rolling elements, the cage, and the inner and outer raceways, thereby conducting a theoretical analysis of rolling bearings. Later, Walters [23] built upon Jones' work to propose a method for the dynamic study of rolling bearings. He further assumed that the motion of the rolling elements was stable and constructed a four-degree-of-freedom dynamic model for the rolling elements. However, during bearing operation, since the motion of the rolling elements is time-varying, the contact angle and centrifugal force change under the influence of varying loads and rotational speeds, rendering this assumption not entirely applicable to the dynamic motion of rolling bearings. Gupta [24] established the generalized differential equations of motion for rolling elements in angular contact ball bearings under viscoelastic conditions. Based on this, he developed a 6-degree-of-freedom bearing dynamics model for the rolling elements, thereby obtaining a comprehensive method for analyzing both transient and steady-state motion of the rolling elements. This method can be used to predict the slippage behavior of ball bearings and the overall motion of rolling elements; however, it does not account for the effects of oil damping and material hysteresis damping, and treats contact conditions such as impact contact as fully elastic contact. Cui Li [25] and colleagues considered the non-smooth behavior of rolling elements. By establishing the dynamic equations of the bearing system, they investigated the factors influencing the dynamic performance of rolling elements under varying bearing structural parameters and operating conditions.

Hirano [26] observed the behavioral characteristics of rolling elements within a bearing by utilizing the phenomenon of magnetic flux changes induced by magnetized balls. The measurement method is shown in Figure 1. The experiment employed a 7307B angular contact ball bearing, and under a pure thrust load, complex three-dimensional motion of the rolling elements was observed. The study indicates that the ratio of the angular velocity of the rolling elements to that of the cage and the inner ring is related to the number of rolling elements, the centrifugal force of each ball, and the magnitude of the thrust load. When the ratio of the thrust load to the centrifugal force is less than 10, the rolling elements will exhibit slippage behavior.

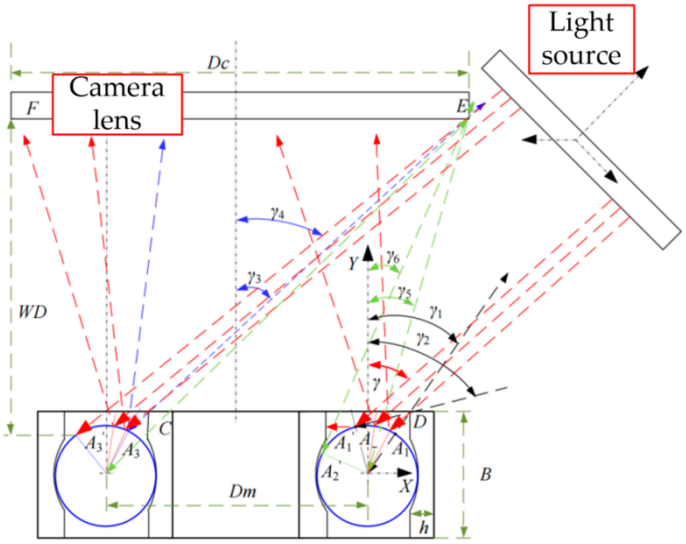


Figure 1. Three-dimensional motion measurement method of rolling elements. Adapted from Ref. [27].

Harris [28], based on the theory of elastic hydrodynamic lubrication, replaced costly testing procedures with a pseudo-static method that accounts for the friction forces acting on the rolling elements and the contact forces between the inner and outer rings to predict the cage rotational speed. He found that rolling element slippage is jointly influenced by the bearing's radial load and the rolling element rotational speed, and established a slippage prediction model based on the time-varying load on the rolling elements. Liao et al. [29], taking into account the centrifugal force acting on ball bearings, analyzed the forces between ball bearing components to determine the contact forces and contact angles between the rolling elements and raceways. They then utilized Hirano's law to study the slippage phenomenon in bearings under combined loads. Tu et al., based on the rolling elements' rotation, revolution, and spin, established a six-degree-of-freedom bearing dynamics model by analyzing the non-smooth contact and slippage behavior between the rolling elements and raceways [30]. Peng et al. performed a force analysis on bearing rolling elements and used a dynamic method to analyze the slippage of three-point contact ball bearings to determine the contact between the rolling elements and the raceways [31]. The analysis indicates that the slippage rate of ball bearings is affected by changes in the contact angle and the actual operating conditions of the bearing. An indirect measurement platform for bearing slippage was constructed, using the variation patterns of the rolling element's inner raceway frequency and orbital rotational speed with respect to axial load and inner raceway rotational speed as the basis for determining bearing slippage. Wang et al. investigated the mechanism of fretting in rolling bearings, analyzed the causes of fretting wear, and, through an established fretting speed model, determined the harm caused by fretting to bearings, providing a theoretical reference for mitigating fretting wear [32]. Ma et al. studied the internal friction heat of bearings by treating the slip within the micro-contact zone as an

input variable [33]. They established a rolling bearing friction heat model that accounts for the slip factor and used the finite element method to model bearing heat generation, as shown in Figure 2.

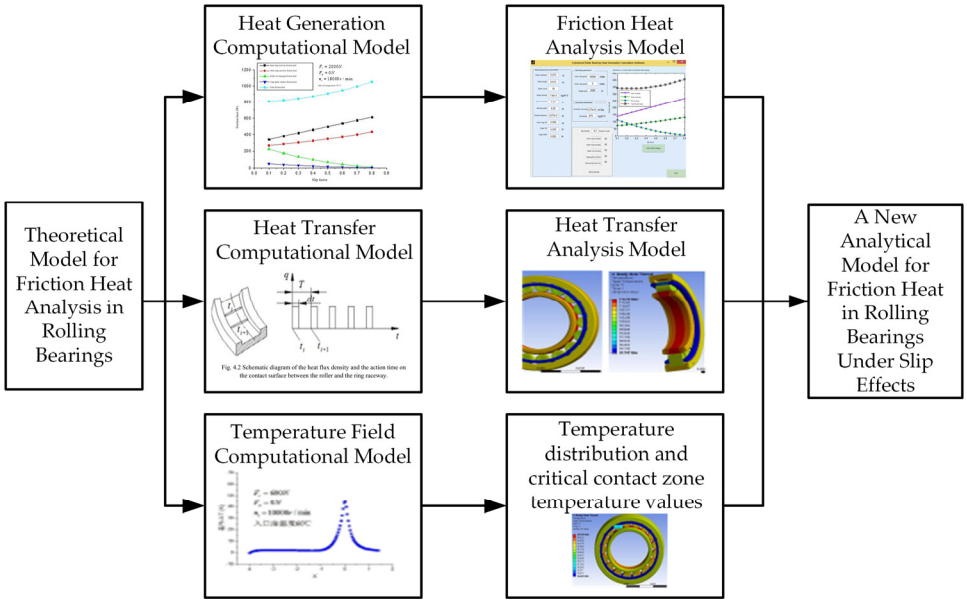


Figure 2. Frictional thermal model of rolling bearings considering slip factor. Adapted from Ref. [33].

The motion of rolling elements is complex and variable, and this behavior is classified as non-smooth. In practical engineering applications, such non-smooth behavior during the motion of rolling elements can affect the fatigue life of bearings. Therefore, analyzing the contact response of raceways to different motion states of rolling elements, controlling the motion of rolling elements, reducing the probability of slippage, and predicting bearing life in practical applications all provide valuable guidance.

2.2. A Study on Non-Smooth Contact Inside Rolling Bearings

The non-smooth behavior of rolling elements results in non-smooth contact between them and the inner and outer raceways. Under no-load conditions, the contact between the rolling elements and the raceways is point contact; as the load increases and the rotational speed rises, this gradually transitions from point contact to line contact [34,35]. The contact area, force distribution, contact stiffness, and contact location all vary with changes in external conditions. This constitutes a boundary non-smooth contact problem, making the non-smooth contact between rolling elements and raceways a major challenge in bearing research [36–38].

Lundberg and Palmgren [39] conducted a theoretical analysis of the pressure distribution in the contact region of rolling bearings, refined Weibull's failure statistics theory, and evaluated the impact of normal loads on the stressed material. They investigated the variables affecting the load-carrying capacity of rolling bearings and, by introducing empirical constants, established a general formula relating these variables to bearing load-carrying capacity, which enables the prediction of the fatigue life of rolling element bearings to a certain extent. Building on this work, Sinha [40] and others improved the calculation accuracy of the contact between rolling elements and inner/outer rings based on the raceway control theory, as shown in Figure 3. Calculations were performed based on the major and minor radii of the contact ellipse, as well as the variation in the position of the contact center under load. Taking into account the deformation of the raceways under

load and the effects of bearing forces, the load distribution within the contact ellipse region, the time-varying contact stiffness, and the contact deformation rate were calculated.

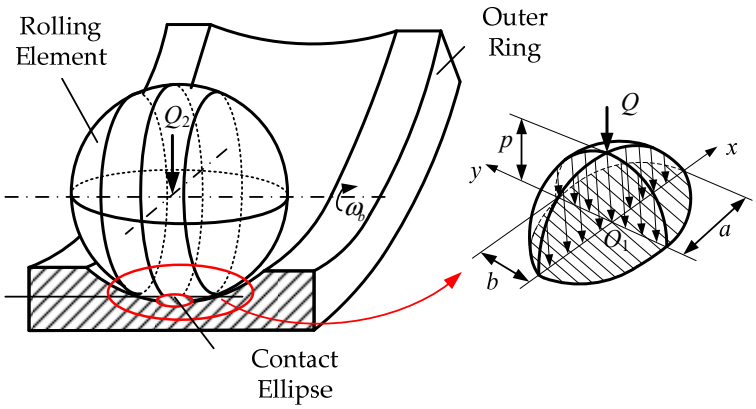


Figure 3. Contact ellipse pressure distribution diagram between rolling elements and raceway. Adapted from Ref. [40].

Ravi S [41] calculated the radial load distribution of the balls based on Hertz's theory of elastic contact. To further investigate the performance of variable-clearance ball bearings, the results were compared with those of conventional ball bearings, revealing that when moving at specific angles on an outer elliptical ring, the combined load on most of the load-bearing balls in the variable-clearance bearing was significantly reduced. Neisi [42] investigated the influence of dimensional tolerances, material properties, and rotor dynamic characteristics on contact stresses in ball bearings. He established models for contact deformation, contact forces, and non-smooth contact stresses within each ball between the ball and the inner ring. The analysis revealed that balls with dimensional deviations alter the contact stiffness between the ball and the raceway, resulting in changes in contact forces and torques. Gao [43] discovered a flutter phenomenon caused by non-smooth ball bearing Hertzian contact during the milling process; that is, under the influence of non-smooth ball bearing Hertzian contact, the milling stability diagram exhibited highly complex dynamic characteristics, resulting in unstable flutter that was even more irregular than the tool helix angle. Zhang [44] and other scholars analyzed the impact of ring misalignment on the operating characteristics of ball bearings. Based on changes in the contact angle, they determined the non-smooth contact state between the balls and raceways, thereby improving the quasi-static model of ball bearings. Building on this model, they analyzed the effect of circumferential misalignment on the stiffness and life of ball bearings under combined loading. Gao [45] established a non-smooth contact model between rolling elements and raceways and presented the results of spindle system vibrations under nonlinear and non-smooth ball bearing stiffness. Within the range of fundamental excitation frequencies ω near the first, second, and third natural frequencies, hardening-type nonlinear behavior was observed, as well as intersections and discontinuities in the frequency response curves.

Guan et al. established a multi-body dynamics model of the rolling elements and raceways under variable-stiffness non-smooth excitation and analyzed the relationship between model stability and various parameters based on numerical simulation methods [46]. Liu et al., taking into account the subtle changes caused by undulations in the non-smooth contact morphology within the oil film contact zone between rolling elements and raceways, proposed a method for rapidly solving dynamic simulation of rough contact surfaces under elastic-fluid lubrication and investigated a nonlinear stress and life prediction model for the sub-surface under elastic-fluid lubrication in non-smooth contact [47]. Liu et al. investigated the relationship between the non-smooth contact characteristics between rolling elements and raceways and localized spalling failures in rolling

bearings [48]. Based on Hertz contact theory, they proposed a non-smooth dynamic model of rolling bearings coupled with time-varying displacement excitation and time-varying contact stiffness excitation. Luo et al. used nonlinear spring and damping components to simulate non-smooth impact contact between the cage and rolling elements [34]. They performed non-smooth dynamic simulations by integrating non-smooth factors such as impact mechanical characteristics, friction, and rotational speed, and analyzed the effects of rotational speed and combined loads on contact characteristics. Tu et al. investigated the internal non-smooth contact characteristics of rolling element bearings under variable load conditions and constructed a rolling bearing dynamic model [49], as shown in Figure 4 [50]. They further explored the patterns of change in contact characteristics between the rolling elements, raceways, and cage when the bearing fails.

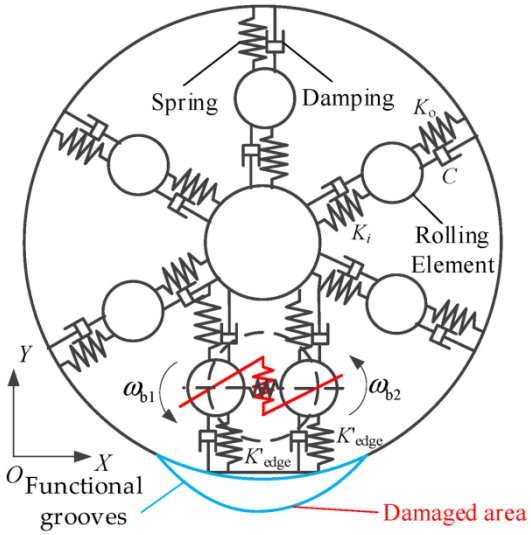


Figure 4. Dynamics model of rolling bearings. Adapted from Ref. [50].

2.3. A Study on the Digital Modeling of Non-Lubricated Behavior in Rolling Bearings

With the rapid development of computer science and hardware and software technologies, research on rolling bearings has gradually shifted from initial experimental and purely theoretical studies toward digital visualization and behavior prediction. To investigate the non-smooth dynamic characteristics of rolling bearings during service and improve the accuracy of computational models, scholars have utilized computer-aided techniques to perform theoretical calculations and establish simulation models for bearings, gradually developing bearing dynamics analysis software to conduct digital simulations and visual analyses of rolling bearings under real-world operating conditions [51–54].

The development of real-time digital dynamic analysis systems for bearings can be traced back to the 1970s, when Walters [55] developed the first computer program, BASDAP, to solve the differential equations of motion between rolling bearing components. Although it simulated the dynamic characteristics of rolling elements and cages, it constrained the interactions between components, resulting in rolling elements and cages having only the same velocity vectors perpendicular to the contact surface. Gupta [56] developed the rolling bearing computer program ADORE, which could simulate the non-smooth dynamic behavior of rolling elements in a six-degree-of-freedom space and reduced the constraints on the cage, thereby accelerating the integration process. This program could account for changes in bearing geometry and the effects of manufacturing tolerances, laying a solid foundation for subsequent scholars to develop and apply digital analysis software for bearings.

Meeks [57] solved the dynamic equations of motion for ball bearings using a six-degree-of-freedom model and vector matrices, as shown in Figure 5. By simulating the inelastic collisions between rolling elements, the cage, and raceways, as well as the slippage of rolling elements, through a computer numerical model, this model can predict dynamic variables such as separator motion, impact forces, and frequencies, as well as acceleration, velocity, and energy losses.

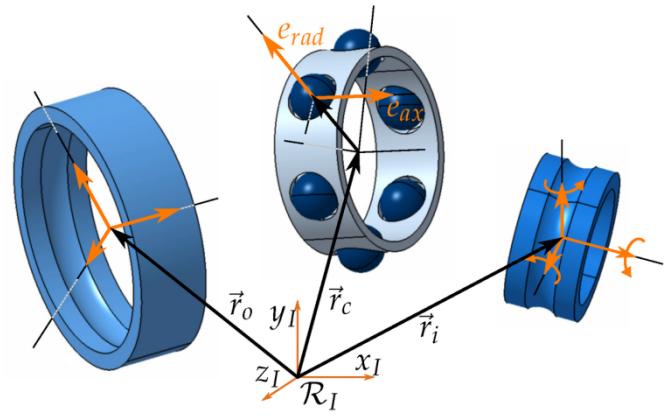


Figure 5. Simulation modeling of ball bearing dynamics. Adapted from Ref. [58].

Houpert [59] proposed a novel method for calculating the equivalent contact stiffness load of rollers and cages, assuming no interference between the roller surfaces and the raceway and cage surfaces. This method combines a nonlinear viscous model to calculate the traction force and incorporates these factors into the development of the bearing dynamics software CAGEDYN. To more closely simulate the non-smooth dynamics of rolling bearings under actual operating conditions, SKF and PELAB jointly developed the BEAST bearing simulation software. This software imposes no constraints on the cage and does not control the rolling elements' movement along the raceways, thereby achieving true non-smooth dynamics simulation. All internal bearing components possess six degrees of freedom, and in subsequent comparisons with experimental data, the results regarding the force and motion parameters of the cage and rolling elements under various load conditions showed excellent agreement [60].

Wang et al. analyzed the dynamic models of rolling elements at different load positions within the bearing, established and solved the non-smooth dynamics equations, determined the motion states of the rolling elements under various load conditions, and proposed the digital program READ, which enables the simulation and characterization of non-smooth behavior in bearings with different structural parameters and varying operating conditions [61]. Zhu used the quasi-Newton method to calculate the maximum contact stress of rolling bearings, corrected the material coefficients of the inner and outer raceways and rolling elements, and obtained virtual prediction results using simulation software [62]. Yan established a dynamic finite element digital model of a rolling bearing in ANSYS Workbench simulation software [63]. By setting spalling failure regions on the outer raceway, inner raceway, and rolling elements of an angular contact ball bearing, he investigated the non-smooth vibration characteristics of ceramic ball bearings exhibiting spalling point failures under specific operating conditions. Wang et al. constructed a digital twin simulation model of a rolling bearing that accounts for surface topography by reconstructing the contact pattern based on point clouds using fractal theory, as shown in Figure 6 [64]. This provides an accurate method for visualizing bearing models to study the non-smooth behavior caused by changes in contact stiffness resulting from bearing surface wear.

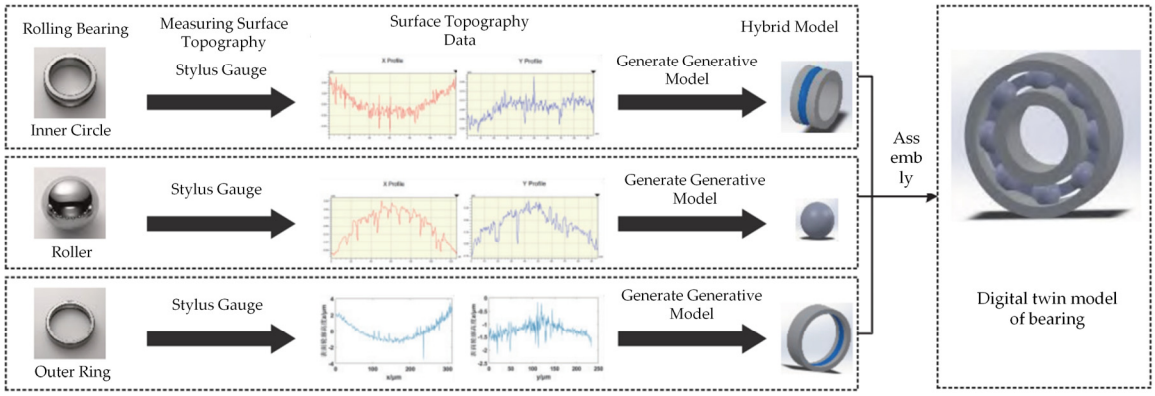


Figure 6. Digital twin modeling of rolling bearings considering surface topography. Adapted from Ref. [64].

2.4. Experimental Study on the Non-Smooth Dynamic Performance of Rolling Bearings

Experimental study is one of the key methods for measuring and verifying the dynamic performance of rolling bearings. Currently, the dynamic performance of non-smooth bearings can be studied using two approaches: direct measurement and indirect measurement [65–67].

Direct measurement allows for the monitoring of bearing service conditions through the direct measurement of temperature and vibration frequency during the experimental process [68–70]. Shiyuan E et al. [71], after considering external excitation forms, made flexibility improvements to the bearing test bench, enabling the measurement results to characterize the life of rolling elements caused by vibration under actual operating conditions such as combined loads. Kumar S A et al. collected relevant parameters through vibration experiments and, by combining them with the underlying abnormal frequency composition and spectral calculations of a visualization interface platform, characterized in real time the abnormal operating frequencies of rolling elements caused by bearing failures, thereby enabling real-time monitoring of the bearing's non-smooth dynamic behavior [72].

Ma et al. addressed the issue of roller slippage by analyzing the relative positional relationship between the rollers and the inner raceway. They derived a formula for calculating the vibration characteristic frequencies of non-smooth motion in rolling bearings [73]. Based on this, they conducted slippage experiments and performed time-frequency domain analysis on the extracted non-smooth vibration signals under pure rolling and slippage conditions. Qiao conducted research on simulation testing technology for fretting wear in rolling bearings, designed a simulation platform for fretting wear experiments, and analyzed the causes of fretting wear in rolling bearings based on the experimental results [74]. Chi optimized the vibration signal transmission process using relevant algorithms to minimize experimental errors, thereby improving the accuracy of rolling element data obtained from subsequent analyses [75]. Tian addressed the issue of heat-induced preload caused by bearing heat generation through real-time simulation [76]. By adding a magnetorheological fluid dynamic loading system to a traditional bearing test bench, he was able to more accurately characterize the non-smooth operational behavior resulting from heat generated by rolling elements and raceways. Pan designed a new experimental setup for testing the dynamic performance of rolling bearings [77]. This setup allows for the comparative analysis of non-smooth dynamic characteristics between rolling elements and raceways with different geometries, providing insights for subsequent performance testing of high-precision rolling bearings under high-speed conditions.

Indirect characterization methods that measure overall bearing motion performance parameters can be used to analyze the non-smooth behavior patterns of rolling elements;

for example, rolling elements can be analyzed by collecting acoustic, optical, electrical, and vibration signals [78]. Based on the traditional theory of raceway-controlled rolling elements, Zhil'nikov et al. [79] proposed a method for calculating the friction torque of caged ball bearings under axial preload by analyzing changes in the contact angle and contact ellipse parameters, as shown in Figure 7. They also compared the maximum friction torque during the operation of caged ball bearings under different axial loads through a combination of experimental and computational analyses.

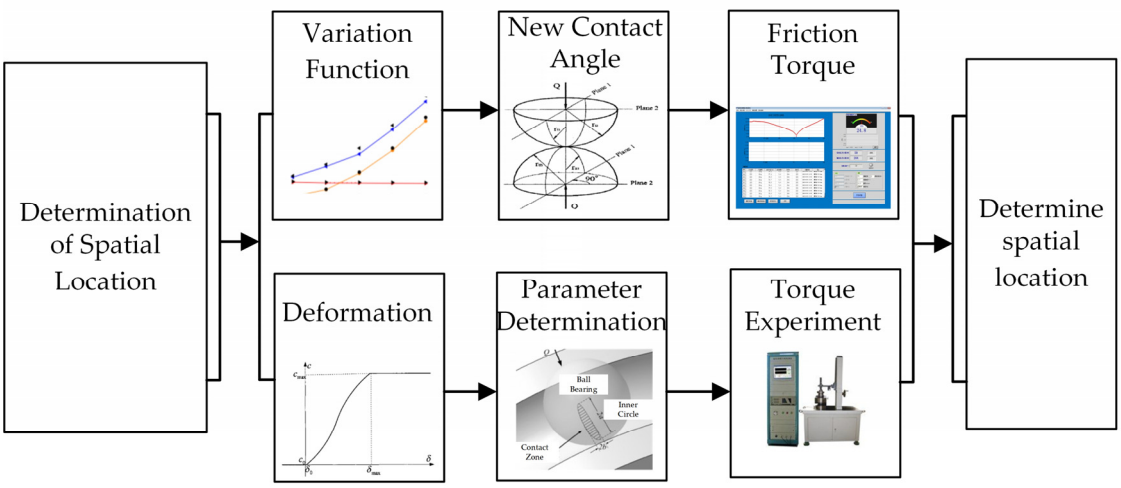


Figure 7. Research process of frictional torque for cageless ball bearings. Adapted from Ref. [79].

Deng Si'er et al. [80] designed a friction torque tester to evaluate the dynamic performance of bearings. To improve the accuracy of transient measurement results, they applied the principle of internal energy conversion within the bearing to achieve non-contact application of the driving torque. Guang et al. designed a dynamic friction torque tester specifically for deep groove ball bearings, capable of automatically detecting friction torque values and evaluating the dynamic performance of rolling bearings based on the range of friction torque variations [81].

Yan et al. measured the sound pressure level of bearing radiation noise using newly added sound pressure sensors, characterizing the relationship between the non-smooth collision behavior of rolling elements and the cage and changes in sound pressure level [27]. Zhao et al. used a high-speed camera to continuously capture images of the rolling elements [82]. After multiple processing steps on the reflective points at the centers of the captured rolling elements, the coordinates of the rolling element centers were obtained, providing data for subsequent calculations of the angular velocity of rotation. Gao, considering that each rolling element in a bearing has non-smooth characteristics, proposed an improved one-dimensional calibration measurement method capable of real-time regression of calibrated rolling element attitude information [83]. Boness R J. [84] and colleagues determined the rolling element's rotation angle and pose by setting capture intervals and fitting the trajectories of light spot formations, thereby generating a continuous sequence of dynamically changing images to assess the rolling element's non-smooth behavior. Han Q [85] and colleagues characterized the time-varying stiffness and vibration patterns of rolling elements under combined loads through experiments on the ratio of radial-to-axial stiffness gradients, combined with the contact angle variation curves and amplitudes between rolling elements and raceways.

The above studies indicate that, to investigate the motion mechanisms and non-smooth contact behavior of rolling bearings in actual operation, scholars both domestically and internationally have simulated actual bearing operating conditions using lumped-parameter

models, quasi-static models, quasi-dynamic models, and dynamic models to study phenomena such as cage slippage, cage impact, and rolling element slippage. However, the constraints in current bearing theoretical models are typically determined by the coupling relationships between components, neglecting the changes in the contact model between rolling elements and bearing components caused by the time-varying nature of the rolling elements' actual working postures. Therefore, building upon the research of the aforementioned scholars, this study examines the non-smooth contact state on the surface of local functional grooves under the combined effects of rolling element rotation, precession, spin, slippage, and fretting, thereby enhancing the accuracy of the established bearing theoretical model.

2.5. Summary and Comparison of the Reviewed Non-Smooth Contact Models

Sections 2.1–2.4 have reviewed the modelling and the experimental characterization of the non-smooth contact response of rolling bearings one study after another. In order to make the comparison explicit, Table 1 summarizes the representative studies in terms of the model or method that is used, the key assumptions on which it rests and the limitations that follow from those assumptions. The table shows that the accuracy of a model is generally paid for by a loss of generality: models that reproduce the full six-degree-of-freedom motion necessarily simplify the contact (elastic, dry and smooth), whereas models that describe the contact in detail are restricted to quasi-static or two-dimensional conditions. It is this trade-off that determines how far the existing models can be extrapolated to the worn, lubricated and colliding contact of the local functional grooves considered in this review.

Table 1. Comparison of representative models and methods for the non-smooth contact response of rolling bearings.

Model or Method (Representative Study)	Key Assumptions	Main Limitations
Quasi-static raceway-control model (Jones [22])	The rolling elements roll purely on the raceway, and the cage and ring geometry control their motion; steady state	Time-varying posture, spin and skidding are neglected
Four-degree-of-freedom dynamic model (Walters [23])	The motion of the rolling elements is assumed to be stable	Not applicable to time-varying speed and load
Six-degree-of-freedom dynamic model (Gupta [24])	Viscoelastic contact; impact treated as fully elastic; oil damping and hysteresis damping neglected	The impact response is overestimated and the damping effects are missing
Magnetic-flux motion measurement (Hirano [26])	Pure thrust load; the measurement itself does not disturb the ball motion	Indirect measurement; single bearing type; no cageless configuration
Pseudo-static skidding prediction (Harris [28])	Elastohydrodynamic contact and friction forces; time-varying load on the rolling element	Steady-state cage-speed prediction; no transient response
Quasi-static combined-load analysis (Liao [29])	Centrifugal force included; empirical skidding criterion	Restricted to ball bearings; the criterion is empirical
Hertzian contact-stress model (Lundberg and Palmgren [39]; Sinha [40])	Elastic Hertzian contact on an ideal smooth surface; empirical life constants	Surface roughness and the lubricant film are neglected
Tolerance- and topography-sensitive contact model (Neisi [42]; Adamczak et al. [86])	Off-sized balls and rigid rings; the surface topography is the source of vibration	No coupling with the bearing dynamics
Misalignment and nonlinear-stiffness model (Zhang et al. [44]; Gao and Meng [45])	Hertzian contact on an idealized geometry	Dry contact; lubrication absent
Rough-surface elastohydrodynamic contact model (Liu et al. [47])	Non-smooth morphology of the oil-film contact zone between the rolling element and the raceway	Limited to subsurface stress and life prediction

Table 1. *Cont.*

Model or Method (Representative Study)	Key Assumptions	Main Limitations
Digital model and digital twin (Wang et al. [61]; Wang et al. [64])	The measured topography determines the contact stiffness through fractal reconstruction	Only the stiffness variation is represented; the damage evolution is absent
Indirect experimental characterization (Zhil'nikov et al. [79]; Gao [83]; Boness et al. [84])	The friction torque or an optical calibration reflects the overall motion of the rolling elements	Indirect, with limited resolution and a limited load range

3. Rolling Bearing Damage Research Methods

Damage to rolling bearings primarily refers to the phenomenon of material spalling caused by relative friction between the rolling elements and the surfaces of the inner and outer raceways. Surface damage to bearings leads to a loss of dimensional accuracy, deformation of the working surfaces, and increased instability in the movement of the rolling elements within the raceways, causing the rolling elements to slip. In severe cases, this can result in the failure of the entire bearing system [87–90].

Khanam et al. [91] pointed out that bearing surface damage generates excitation forces, the magnitude and timing of which are related to the size of the damaged area. Based on this, they proposed an impact function for rolling elements passing through the damaged area, as well as the relationship between post-damage stiffness variation and the motion state of the rolling elements. To investigate surface damage excitation in ceramic ball bearings, Zhang et al. [92] installed three types of hybrid ceramic ball bearings on the same spindle of a bearing test rig and conducted comparative experiments under identical conditions. The results showed that the surface fatigue behavior of ceramic balls differs from that of traditional rolling contact fatigue, and that hard particles detached from the ceramic ball surface formed a large number of micro-pits on the raceway surface under compressive forces. Guan Zhenzhen et al. [93], combining the clearance patterns generated by rolling element motion, used time-varying Hertzian contact forces as parameters for the damage excitation function to establish and solve the multi-degree-of-freedom damage vibration differential equations of the bearing system. Chen Guo [94] analyzed factors such as the clearance between the rolling elements and raceways after damage, non-smooth contact deformation, and flexible vibration of rolling bearings. Based on this analysis, a segmented damage excitation dynamic model was established for different damage scenarios, leading to a damage model describing the dynamic response of a rotor system under unbalanced coupling, as shown in Figure 8.

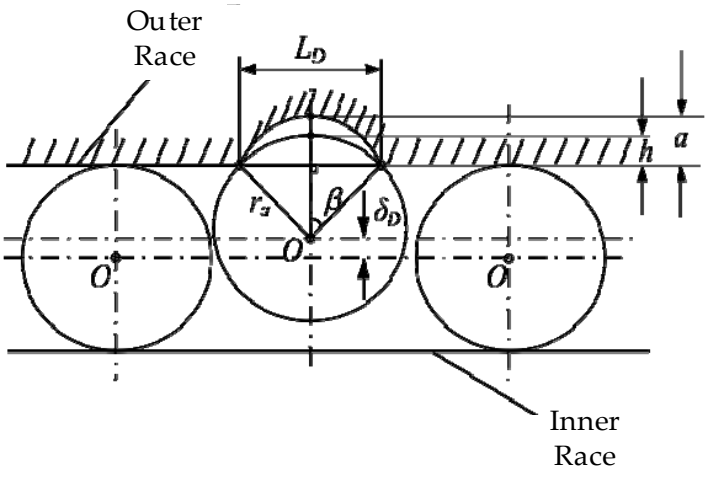


Figure 8. Damage model of dynamic response law of rotor system. Adapted from Ref. [94].

Most of the aforementioned research simplifies bearing damage excitation to a pulse signal; however, virtually no studies have examined the effects of three-dimensional spatial variations in damage, which does not fully align with actual operating conditions. As rolling elements pass over damaged areas, contact conditions vary; furthermore, the damage propagation process during high-frequency passage further alters the damage excitation pattern, thereby affecting the vibration modeling and theoretical analysis of bearing damage.

Adamczak et al. [86] argue that using only two-dimensional topography parameters is insufficient to describe the surface topography of damaged bearing raceways. Based on extensive measurements of damaged rolling bearing surfaces, combined with dynamic vibration results of rolling elements, they contend that it is necessary to employ three-dimensional topography parameters in theoretical research to provide a more detailed description of the damaged raceway surface topography, thereby ensuring greater accuracy in research results. Zheng et al. used ABAQUS simulation software to analyze the stress distribution at the contact points between various rolling bearing components, established a three-dimensional damage model of the bearing components, and predicted the bearing's fatigue life based on this model [95]. Yang, in order to study the characteristics of the outer raceway of aircraft engine bearings, employed lubricant spectroscopy, portable ferrography, analytical ferrography, and energy spectroscopy techniques to analyze abrasive particles in the bearing's internal lubricant [96]. He found that spalling propagation on the outer ring of ball bearings is progressive; damage to the outer raceway first appears at a certain distance behind the pit and propagates along the rolling direction of the rolling elements. Luo et al. analyzed the time-varying displacement excitation at the contact between the rolling element and the damaged region [97]. By calculating the energy of the bearing system at both ends of the damaged region, they derived a model for the force and damage length when the rolling element impacts the damaged region. Introducing the damage function into the dynamic equations, they established a dynamic model for bearing impact damage. The analysis showed that the bearing vibration amplitude exhibits a double-impact phenomenon when the rolling element enters and exits the damaged region.

Imran [98] proposed a research method based on dimensionless amplitude response analysis and scaling laws, incorporating parameters such as bearing damage volume and the surface area of the damaged region to evaluate the relevant characteristics of damage in different components of rolling contact bearings within a dimensionless-scaled rotor–bearing system. Lu Yang [99] conducted modeling and simulation of the damage failure dynamics of deep-groove ball bearings, incorporating the geometric parameters of the damaged region into the established single-point-failure bearing dynamics model. Smith et al. [100], after comprehensively analyzing the effects of bearing geometry, rotational speed, combined loads, and vibration damping, proposed converting the vibration signals from the local damage zone into impulse excitation and transforming the damage factors into rolling element impulse signals for bearing dynamic modeling. Fan et al. [101] calculated the additional contact deformation of rolling bearings caused by damage based on the unbalanced internal forces resulting from damage to the inner and outer raceways, established a six-degree-of-freedom vibrational differential model, and found through solution that the unbalanced forces caused by damage to the inner and outer raceways have a significant impact on the vibration amplitude of the bearing. Behzad et al. [102] proposed characterizing local bearing damage as random variations in surface roughness amplitude within a certain range, with this random distribution conforming to a Poisson distribution. Liu et al. [103] proposed a new model of time-varying contact forces, contact deformations, and non-smooth contact relationships between rolling elements and the edges of raceway damage, thereby deriving the relationship between time-varying

contact stiffness and damage dimensions. Jiang et al. [104] found in their study that the dimensions of the edges of the raceway damage zone are related to changes in the rolling element's radius of gyration, the depth of the damage zone, and the span angle, and based on this, they established a three-dimensional model of a bearing with a local damage zone. Figure 9 shows the relative displacement diagram of the rolling element passing through the damage zone.

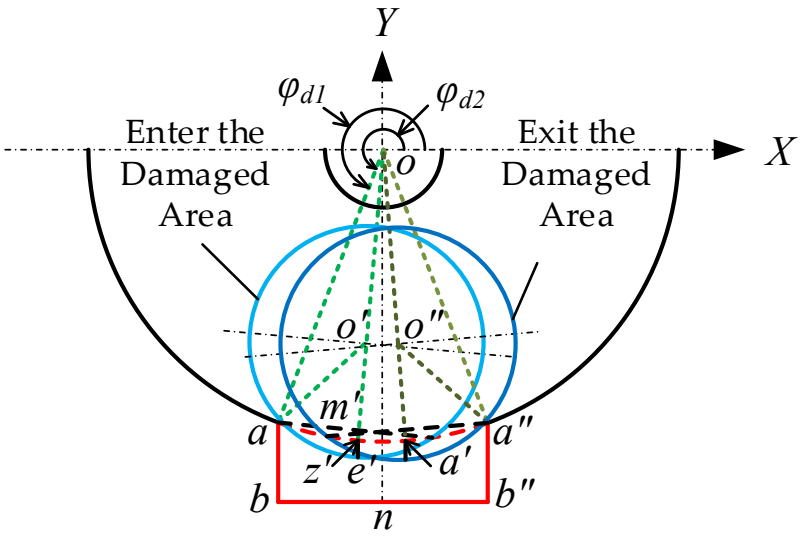


Figure 9. Relative displacement diagram of the rolling element passing through the damaged area. Adapted from Ref. [104].

Ghezzi et al. [105] reproduced the damage patterns of oscillating grease-lubricated hybrid bearings under high radial loads. They conducted SEM analysis of the raceways after the micro-running-in phase, focusing on the evolution of the damaged contact surfaces, and compared these findings with macroscopic observations of changes in the rolling element morphology. Lai [106] demonstrated that geometric deviations in the bearing housing can induce tensile stresses near the raceways. These tensile stresses promote the propagation of subsurface cracks toward the raceways, leading to surface fracture cracks or axial cracks, which in turn cause internal damage to the bearing. Most researchers have focused solely on the mechanics of bearings to investigate internal conditions and the impact of damage on dynamic performance, without conducting direct studies at the material or microscopic levels. Chiu et al. [107] proposed a statistical model for the origin of subsurface cracks at bearing contact points; weak areas in the bearing raceway material are prone to cracking, and the material's physical properties and coefficient of friction determine the extent of damage to rolling bearings. Lian [108] proposed a thermomechanical phase transformation finite element method to quantitatively predict the formation process of thermally induced white etching layers on raceway surfaces. Yan [109] conducted a systematic analysis of rolling and sliding contact fatigue failure on the surface of AISI 9310 bearing steel, examining the evolution of fatigue life, microstructure, and crystal orientation, as well as changes in microhardness and residual stress distribution. Ren [110] characterized and reconstructed the three-dimensional geometric structure of bearing damage based on experimental statistics. The three-dimensional superposition of fracture modes enables more accurate prediction of RCF crack propagation paths and reveals the propagation mechanisms of cracks in both the contact surface and subsurface regions.

Tallian [111,112] established a fatigue life prediction model for rolling bearings by statistically analyzing the distribution of surface damage severity across different bearing locations. This model uses the physical parameters of the bearing surface material, orthog-

onal shear stress under fatigue conditions, and parameters related to damage severity as primary variables to calculate fatigue life as the lifespan under this stress field. Few models link the micro-mechanical behavior of materials to the damage behavior of rolling bearings. The first fatigue crack appears at a weak point in the material and always manifests as a microcrack; the micro-physical properties of the material influence the initiation of bearing damage. Therefore, when studying bearing damage, one must not only consider the establishment of macroscopic models but also investigate the fundamental causes of crack initiation at the micro-scale [113–115].

Based on the aforementioned research, it can be observed that rolling bearing damage results from the combined effects of multiple factors and is influenced by load, rotational speed, lubrication, and environmental conditions. Researchers generally employ two approaches to study bearing surfaces: one involves establishing vibration excitation to assess the extent of bearing damage, and the other involves constructing the geometric morphology of the damaged surface to predict the bearing's fatigue life. Existing bearing research often focuses on macroscopic forces, contact deformation, or the material itself; however, studies conducted from a single perspective or scale cannot accurately characterize the operating conditions of bearings during operation. Therefore, it is essential to conduct multi-scale, multi-factor research on damage mechanisms.

As in Section 2, the studies reviewed above are compared in Table 2 in terms of the assumption on which each method rests and of the limitation that follows from it. The comparison shows that the methods used to research bearing damage fall into two families: those that treat the damage as a source of vibration excitation with an idealized geometry, and those that describe the damage geometry in detail but do not couple it to the dynamics of the bearing. Very few approaches relate the three-dimensional, time-evolving damage of the raceway to the dynamic response of the bearing, which is precisely the problem of interest for a worn local functional groove.

Table 2. Comparison of representative methods for rolling bearing damage research.

Method (Representative Study)	Key Assumptions	Main Limitations
Impact-excitation model (Khanam et al. [91])	The damage excitation is a pulse whose amplitude is proportional to the size of the damaged area	The three-dimensional morphology and the wear evolution of the damage are lost
Damage-vibration model (Guan et al. [93]; Chen [94])	A time-varying Hertzian contact force or a segmented excitation function represents the damage	Idealized damage geometry; simplified rotor coupling
Topography-based damage assessment (Adamczak et al. [86])	The two- and three-dimensional topography parameters dominate the vibration level	No dynamic model and no damage prediction
Finite-element damage and fatigue-life model (Zheng et al. [95])	Elastic material; static stress field; the damage geometry is taken from the measurement	No dynamics, no lubrication and no wear evolution
Debris and ferrography analysis (Yang [96])	The spalling propagates progressively and is reflected in the debris of the lubricant	Offline and qualitative
Time-varying displacement-excitation model (Luo et al. [97]; Jiang et al. [104])	The rolling element is displaced by an idealized defect profile, with a double impact at the entry and the exit	Idealized geometry, no lubrication, and no wear evolution
Dimensionless amplitude and scaling model (Imran [98])	The damage volume and the damaged area are the governing scaling parameters	Requires calibration against experiments
Time-varying contact-stiffness model (Liu et al. [103])	Dry elastic contact; the stiffness is determined by the damage dimension	Not verified experimentally

Table 2. *Cont.*

Method (Representative Study)	Key Assumptions	Main Limitations
Grease-lubricated damage reproduction (Ghezzi et al. [105])	The damage morphology after the micro-running-in phase represents the service damage	One operating condition; no vibration model
Material-level damage analysis (Lai [106]; Chiu et al. [107]; Lian [108]; Yan [109]; Ren [110])	The damage is controlled by the microstructure, the residual stress and the crack initiation at the material scale	Not connected to the bearing-level dynamics
Statistical fatigue-life model (Tallian [111,112])	The damage severity follows a statistical distribution and empirical constants are used	No local damage geometry and no dynamics

4. Mesoscopic Damage Characterization Methods

Surface damage in bearings is primarily caused by cyclic friction between the rolling elements and the raceways. With the advancement and application of tribology theory, research on bearing surface friction and wear has gradually shifted from the macroscopic scale to the microscopic scale, and a combined multiscale approach enables more accurate modeling. Tribological modeling is categorized into continuous and discrete mechanical methods, as well as multiscale approaches, each suited for simulating different time and length scales, as shown in Figure 10. These include the finite element and boundary element methods, discrete dislocation dynamics and molecular dynamics methods, and multiscale methods [116].

In continuum mechanics, the primary methods are the finite element method and the boundary element method. Their relationship can be defined in infinitesimal or finite strain formulations, enabling the modeling of any constitutive material ranging from simple linear elasticity to complex crystalline plasticity [117–120]. The boundary element method employs basic solutions for normal and tangential point forces in its formulations, thereby linking surface traction to surface displacement [121–124]. Discrete dislocation dynamics is a modeling technique for studying plasticity at the microscale; for contact problems, rough surfaces require fine discretization, making other discrete element methods more efficient [125–127]. Macroscopic behavior depends both on the physical properties of individual particles and on the interactions between them. The discrete element method (EDEM) is an ideal approach for solving these contact configurations because it allows the physical state of the system to be described using a large number of discrete elements, with particles governed by constitutive equations rather than interactions [128–130]. The discrete element method overcomes the shortcomings of the macroscopic continuity assumption in traditional continuum mechanics models. It enables the study of friction and wear processes on the outer raceway surface of bearings and characterizes their macroscopic wear behavior by analyzing changes in contact forces between particles. Therefore, this paper primarily employs the discrete element method to investigate the damage mechanisms in the local functional groove regions of bearings.

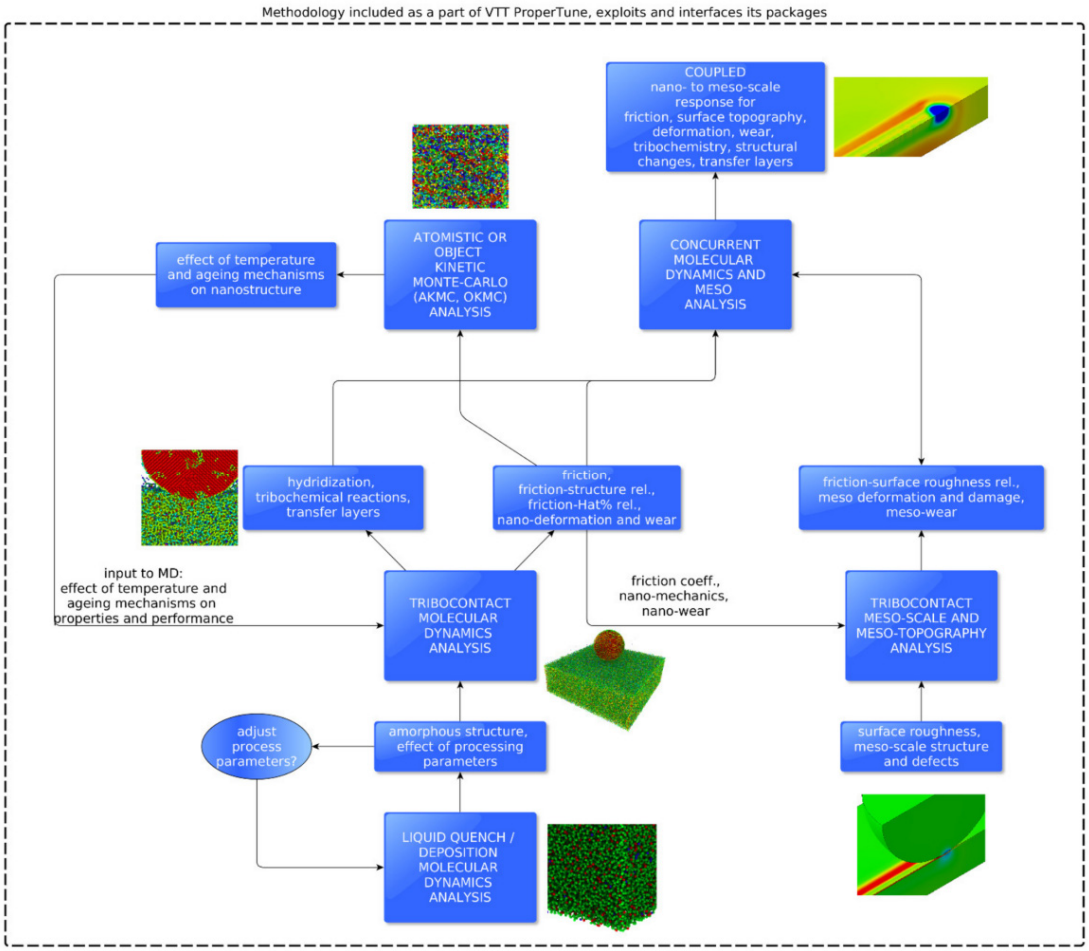


Figure 10. A representative tribological modeling approach built across scales. Adapted from Ref. [131].

In the study of discrete particles, their mechanical behavior is analyzed at three scales, (a) macroscopic scale, (b) mesoscopic scale, and (c) microscopic scale, as shown in Figure 11 [132]. At the microscopic scale, each discrete material particle or aggregate of discrete particles possesses both translational and independent rotational degrees of freedom. These particles can both receive torque couples from other discrete material particles or aggregates and transmit torque couples through mutual contact points.

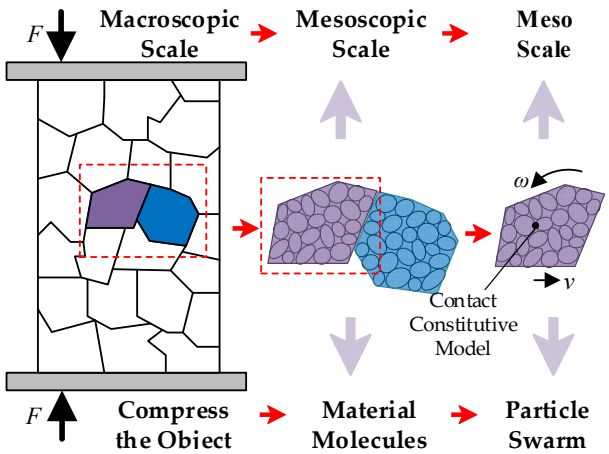


Figure 11. Discrete element scaling. Adapted from Ref. [132].

4.1. Modeling and Simulation Using the Discrete Element Method

Macroscopic wear behavior depends not only on the physical properties of microscopic particles but also on their interactions. To apply the discrete element method (DEM) to establish a mesoscale constitutive model of localized functional grooves and thus analyze the mesoscale damage trends in bearings, it is necessary to conduct in-depth research on the fracture of bonds resulting from contact and motion between discrete particle clusters, as well as the influence of macroscopic damage surface topography on the geometric dimensions of these clusters.

The EDEM method, first proposed by Cundall and Strack [133], is an ideal approach for handling these inter-particle contact configurations, as it allows the use of a large number of discrete elements to describe the physical state of the system. This method employs a soft-ball particle model, in which particles undergo compression and collision, resulting in a certain degree of overlap. It then calculates the contact forces between particles and, by quantifying the interaction relationships among particle force, velocity, and displacement, proposes various contact deformation models between particles, as shown in Figure 12.

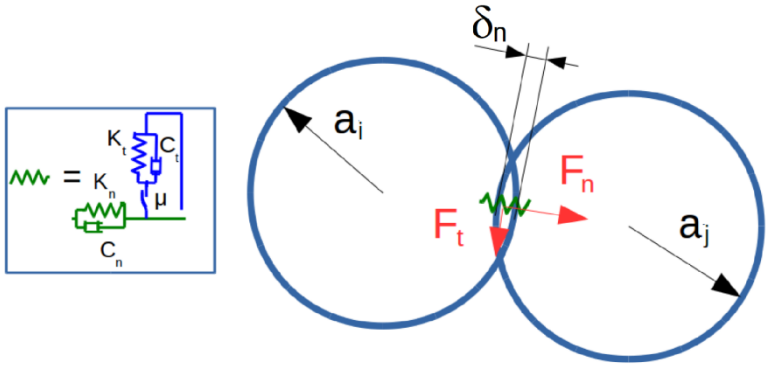


Figure 12. Contact deformation model between particles. Adapted from Ref. [134].

Lu [135] modified Maugis's extended solution of the Johnson–Kendall–Roberts (JKR) theory of adhesive contact for exact spherical contact, defining the interfacial adhesive energy over the actual spherical contact area rather than its projected plane. Lu and Third [136] reviewed progress in the development and implementation of ellipsoidal particle models, as well as algorithms for effective contact detection and the determination of contact parameters. Most of the structures studied are irregular, and calculations using traditional spherical particles cannot accurately describe material properties [137,138]. Acevedo [139] characterized the morphology of deposits based on the aspect ratio and feed rate of the particles, then experimentally validated a discrete element method based on spherical polygons, presenting experimental and numerical results on particle arrangement and stress distribution in sheet-like granular fillers deposited in small-scale two-dimensional silos. Donev [140] proposed a systematic algorithm applicable to hard ellipsoids and ellipsoids. Unlike other microscopic research methods, the discrete element method studies particle contact states by establishing constitutive models between particles. Wachem [141] derived a new framework using unit quaternion transformation vectors and tensors to calculate particle rotation matrices, established particle motion models through motion pose transformations, and thus calculated particle angular and linear velocities at different time points. The particle spatial transformation coordinate system is shown in Figure 13.

Chen [142] employed a time-domain homogenization method to propose a linear viscoelastic constitutive model for particle-reinforced composites based on micromechanics. After decomposing particle contact deformation into volume and displacement components, the author derived an effective constitutive model for the composite and investigated

the effects of particle volume fraction, strain rate, and viscoelastic parameters on the composite's effective viscoelastic behavior and creep properties. Song [143] proposed a new constitutive model for magnetorheological polishing fluids (MRPFs) based on the hexagonal close-packed structure of magnetorheological fluids (MRFs) to predict relevant properties such as the yield shear stress field. Since particle media possess complex characteristics distinct from those of continuous media, statics cannot fully describe the state of particles; therefore, research into particle motion is essential. Mandø and Rosendahl [144] summarized existing methods for modeling the motion of ellipsoidal particles under high Reynolds numbers within the Eulerian–Lagrangian framework for dispersed flow.

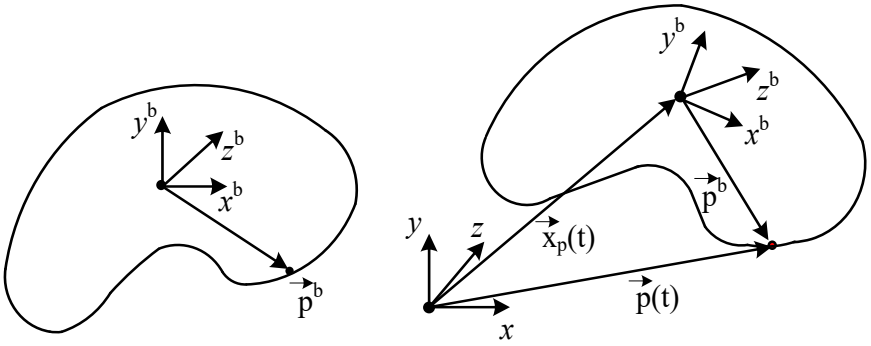


Figure 13. Particle space transformation coordinate system. Adapted from Ref. [141].

The application of the Discrete Element Method (DEM) has expanded from its initial focus on geomechanics to the field of mechanical engineering, where it is widely used in wear research. Yin et al. [145] combined the finite element method with the Discrete Element Method to perform simulation analysis of wear in ball mill elevators. The simulation results predicted the wear distribution of the elevator, providing a theoretical foundation for subsequent efforts to reduce wear. Chen et al. [146] employed the discrete element method to simulate pin-and-disc wear experiments in order to predict the sliding wear of individual iron ore particles, using the contact model within the discrete element method to simulate the interactions between particles and geometric bodies. Some researchers have utilized the bonding model in the discrete element method to discretize a continuum and predict continuum wear. Nguyen et al. [147] used the discrete element method to perform numerical simulations of the wear and fragmentation of agglomerates in a diffusion mixer, distinguishing between wear and fragmentation behavior by comparing the reduction in agglomerate size caused by bond failure with the reduction calculated based on individual particles. Luo et al. [148] used a custom-built experimental setup to measure the discrete element parameters of ellipsoidal pellets and analyzed the effects of different calcination temperatures and equivalent diameters on these parameters. Additionally, they measured and extracted the wear rates and movement velocities of different pellets within a drum. Luo [149] employed a discrete element numerical simulation method to investigate the evolution of tool wear during the machining of high-temperature alloys. Based on boundary conditions, a discrete element model of tool-chip wear behavior was established, and the number of microcracks, the number of detached particles, and the wear rate of ceramic tools were predicted and analyzed through discrete element simulation. Fang et al. [150] proposed a method for predicting the evolution of structural boundary wear based on the discrete element method. They represented the worn structural boundary using spherical boundary elements and reduced the computational load of the discrete element simulation by converting the contact detection between the structural boundary and particles into contact detection between the spherical boundary elements and particles. Zhang et al. [151,152] constructed a mechanical model of the wear-resistant body surface

based on the discrete element method. Using discrete element software, they established structural models of the wear-resistant surface and its abrasive wear system, including step, convexity, and flake arrangement structures. Through qualitative analysis of abrasive particle morphology, contact-bonding fields, and contact force chains, they observed minor damage and detachment phenomena in the abrasive wear behavior.

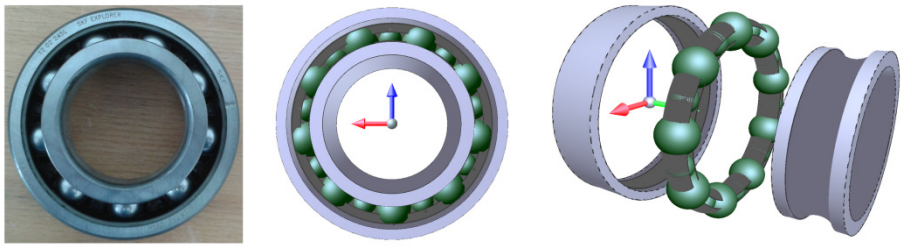
4.2. Applications of the Finite Element Method in the Bearing Industry

In previous studies, multiscale modeling has gradually been applied to the field of bearing wear research. Li [153] used scanning electron microscopy and laser 3D microimaging techniques to measure the friction coefficients and wear rates of sliding bearings under various operating conditions and to examine the wear surfaces of the bearings. Zhang [154] conducted a microscopic analysis of slippage, discovering a large number of pits and microcracks of varying sizes on the surface of the damage zone. Based on topographic maps of cross-sections from the bearing damage area, he inferred the spalling formation process in cylindrical roller bearings. Zhao [155] discretized the rolling elements and outer ring of a cage-less ball bearing into a particle system connected by adhesive bonds. He analyzed the contact states and forms between particles in the outer raceway, established a contact mechanics model for the particles, and derived the energy conservation equation for the particle system based on its arrangement. This allowed him to determine the variation patterns of external forces acting on the rolling elements and different bearing position elements.

Some researchers have employed the discrete element method to investigate bearing damage mechanisms. Bourbatache [156] developed a two-dimensional discrete element model of a ball bearing, monitored ball bearing contact, and calculated the contact forces, velocities, and positions of different elements within the multi-contact system. By analyzing the influence of particle angular velocities in the discrete element model on electrical signals, he derived a predictive model for comparing the sensitivity of local bearing damage detection. Wan Yaqing [157] monitored the movement trends of discrete particles on the surface of rolling bearings and concluded that the damage trends of rolling bearings align with the movement directions of these discrete particles. Guo Shihui [158] established a discrete element dynamic model of a rotor system. The motion state and degrees of freedom of the discrete elements in the model are not affected by the complex motion within the rotor system, providing an innovative and efficient numerical calculation method for the dynamic analysis of multi-body systems. Villavicencio et al. [159] used the discrete element method to investigate the influence of the microstructure of composite materials in rolling bearing cages on the occurrence of crack damage in the cages. By applying specific forces and velocities to the discrete element model of the cage, they simulated the interaction between the rolling elements and the cage. The results indicated that the shorter the fiber length, the easier it is for particle interactions to be disrupted, and the more susceptible the cage is to damage. Machado et al. [160–162] established a discrete element model of a bearing in a two-dimensional simulation, as shown in Figure 14. In the model, in addition to rolling elements and cages being modeled as particles, the inner and outer rings of the bearing were also discretized into a combination of viscous particles. By introducing an electromechanical coupling method, the relationship between the bearing's dynamic mechanical state and electrical signals was simulated, and the bearing's lubrication state was predicted to improve bearing life.

The mesoscopic damage characterization methods discussed above are compared in Table 3. The comparison makes clear that no single method covers the whole range of scales that is involved in the damage of a local functional groove: the continuum methods are efficient but cannot describe the detachment of material; the molecular and dislocation

methods describe the physical mechanisms but are restricted to extremely small domains; and the discrete element method occupies the meso-scale position that is required here, at the price of empirical contact and bond parameters that have to be calibrated. Multiscale coupling is therefore the natural direction of the next step, as discussed in Section 6.



(**a**) (**b**) (**c**)

Figure 14. Discrete element model of bearings: (**a**) the ball bearing; (**b**) two-dimensional discrete element model; (**c**) three-dimensional discrete element model. Adapted from Ref. [134].

Table 3. Comparison of mesoscopic damage characterization methods.

Method	Length Scale	Core Advantage	Main Limitation
Finite element method [117–120]	Continuum, macro–meso	Mature and versatile; arbitrary constitutive models and multiphysics coupling	Mesh dependence; difficult to describe particle detachment and fracture
Boundary element method [121–124]	Continuum, macro–meso	Fundamental solutions reduce the problem to the boundary; accurate for half-space contact	Difficult for inhomogeneous and plastic materials
Discrete dislocation dynamics [125–127]	Micro	Reproduces plastic deformation and the interaction of dislocations	Very high computational cost and a very small domain
Molecular dynamics [130]	Nano–micro	Reveals the atomistic mechanisms of friction, adhesion and wear	Extremely small length and time scales; empirical potentials
Discrete element method [128,129,133]	Meso	Contact and bond constitutive laws give access to particle-scale fracture and wear evolution	Empirical contact parameters, calibration effort and high cost for large systems
Multiscale coupling [116]	Across scales	Combines the accuracy of the fine scale with the efficiency of the coarse scale	Consistency of the interface and of the parameter transfer

5. Discussion

In contrast to Sections 2–4, which are devoted to an overview of the state of the art, this section provides a critical discussion of the reviewed work. It clarifies two concepts that are frequently used in an ambiguous manner in the literature, namely the non-smooth surface and the role of the lubricant; it compares the reviewed models and methods explicitly; and it states the limitations of the existing studies and of the present work. The models and methods discussed in Sections 2–4 are summarized and compared in Tables 1–3, in which the key assumptions and the main limitations of each category are listed explicitly.

5.1. Clarification of the Concept and Manifestations of Non-Smooth Surfaces

In an ideal sense, no engineering surface is absolutely smooth. The concept of a non-smooth surface refers to a solid surface whose geometry deviates from the ideal nominal (mathematically smooth) form over a broad range of length scales, that is, form error, waviness, roughness and deliberately manufactured discrete features such as grooves, dimples, dents and bumps [47,86,116,123]. The non-smoothness of a surface is therefore not a defect

but an intrinsic attribute of a real tribological interface: the smaller the observation scale, the more evident the non-smoothness becomes. For rolling bearings, the non-smoothness of the raceways, of the rolling elements and, in the case considered here, of the local functional grooves is the physical origin of the non-smooth contact response reviewed in Section 2.

The manifestations of surface non-smoothness in rolling bearings can be classified into three levels. (i) The geometric manifestation is the multi-scale deviation of the surface from the ideal form, comprising roughness, waviness, form error and deterministic textures or defects [86,123]. (ii) The mechanical manifestation is the discontinuous or strongly nonlinear variation in the contact area, contact force, contact stiffness and friction coefficient when the rolling elements sweep across such a surface [47,116]. (iii) The dynamic manifestation is the discontinuity, stick–slip and impact behaviour of the motion states of the rolling elements (orbital revolution, rotation, spin, skidding and fretting), which is exactly what is termed non-smooth behaviour in Sections 2.1 and 2.2. The local functional groove studied in this review is a typical artificially introduced non-smooth surface feature: it is designed to interrupt the otherwise smooth raceway so as to differentiate the orbital velocities of adjacent rolling elements. Once the groove is worn, however, the deliberately designed non-smoothness is progressively replaced by a damage-dominated non-smoothness, which is the reason why the two aspects cannot be treated separately.

Once the multi-scale nature of surface non-smoothness is recognized, the influence of surface textures deserves particular attention, because a texture is the most controllable way of tailoring the non-smoothness of a surface. Extensive studies have shown that a properly designed surface texture can (a) act as a micro-reservoir that retains lubricant and re-supplies the contact under starved lubrication, (b) trap wear debris and thus reduce abrasive damage, and (c) generate additional hydrodynamic pressure so that the load-carrying capacity increases and the friction coefficient and the friction torque decrease [163–165]. Because the contact pressure, the film thickness and the asperity interaction are all modified by the texture, the friction-induced vibration and the overall vibration level of the textured bearing are changed as well: a properly selected texture reduces the vibration level, whereas an improper geometry aggravates it [164,166]. For dry and starved contacts, which are the conditions closest to the protection state of a cageless backup bearing, the texture effect is strongly geometry-dependent: dent textures may reduce the friction coefficient and the wear rate, but a depth or a density that is too large causes stress concentration and film rupture [165,167]. Textures are therefore not unconditionally beneficial, and the benefit can only be judged from the specific geometry and the lubrication state [168]. Similar conclusions have been drawn for the influence of deterministic textures on the load-carrying capacity of conformal contacts [169], for vein-bionic textures on cylindrical roller thrust bearings [170] and for the reduction in the vibration level by surface texturing in journal bearings [69]. Accordingly, the design of a local functional groove should be treated as a surface-texture design problem: the depth, width, edge radius, spacing and areal density of the grooves govern both the self-dispersing effect and the damage evolution, and they should be optimized rather than selected empirically.

5.2. Influence of the Lubricating Oil/Grease and of Its Water Content

The discussion would not be complete without considering lubrication, because the dry-friction condition assumed in most of the reviewed models and in the present experimental verification is only a bounding case. In an actual support or protection bearing a lubricating oil or grease is almost always present between the rolling elements and the raceway, and an elastohydrodynamic (EHL) film of the order of the surface roughness is formed. The most direct consequence is that the hydrodynamic pressure and the accompanying squeeze-film damping separate the contacting bodies, suppress the impact pulses

and the oscillations of the rolling elements, and thus change the vibration signature that is used to identify damage; this has been demonstrated theoretically and experimentally on preloaded EHL angular contact ball bearings [67]. The film thickness and the traction are governed by the viscosity of the lubricant, which decreases as the temperature rises; at high speed the film becomes thinner while the temperature rise further decreases the viscosity, so that the lubrication regime shifts from full film towards mixed or even starved conditions [171]. Under starved EHL conditions the film thickness is controlled by the rate at which the oil is supplied rather than by the fully flooded theory, so that the film may collapse locally, asperity contact occurs and the friction, wear and temperature rise increase [172]. Dynamic simulations of EHL ball bearings further show that the lubrication state can itself excite additional vibration of the rotor–bearing system, which indicates that the lubricant is not merely a passive damping element but takes part in the non-smooth dynamic response [173].

Grease is the most widely used lubricant in rolling bearings, and its lubrication mechanism differs from that of oil. Grease is released gradually from the thickener matrix and is replenished by the reflow of the residual layer; when the reflow is too slow, the contact starves and the film thickness falls to a small fraction of the fully flooded value [174]. The friction in a grease-lubricated contact depends on the composition of the grease, that is, on the base-oil viscosity, the thickener type and the additive package, rather than on the base oil alone [175]. The film thickness is further affected by mechanical ageing: after prolonged running the thickener structure is degraded, the film becomes thinner and less stable, and the friction torque and the temperature rise increase [176]. For the cageless ball bearing used as a backup bearing for active magnetic bearings, in which the rolling elements collide repeatedly, the grease is subjected to strong shear and to a considerable temperature rise, so that the mechanisms mentioned above (bleed, reflow, starvation and ageing) determine whether the collision-induced vibration is damped or amplified.

The water content of the grease is one of the most important, and most frequently neglected, factors of grease performance. Water entering the contact (through condensation, a humid environment, water-based contamination or cleaning) changes the microstructure of the thickener: the soap fibres of a calcium sulfonate complex grease swell and reorganize in the presence of water [177], which changes the apparent viscosity and the rheological behaviour of the grease [178] and reduces the EHL film thickness formed in the rolling contact [179]. Water contamination also lowers the shear stability of the grease, so that the grease degrades faster and loses both its consistency and its ability to be replenished at the contact [180]; together with the corrosion of the bearing surfaces, this leads to premature failure. A comprehensive review of grease water resistance shows that the water content that can be tolerated depends on the type of thickener, and that the failure modes range from film collapse and increased friction to corrosion and to the softening or hardening of the grease [181]. A recent study of a calcium-based grease contaminated by both SiO_2 particles and water reports a combined degradation of the penetration, the dropping point and the friction torque that is more severe than that caused by either contaminant alone [182]. Since the grease of a backup bearing of a magnetic-bearing system may contain a certain amount of water after long-term service, the water content should be treated as a state variable of the protective bearing, and the film thickness, the friction torque and the vibration level should be evaluated as functions of it.

The above discussion has two implications for the present review. First, the dry-friction assumption adopted in the reviewed models and in the dry-friction tests of local functional grooves gives the most severe, upper-bound contact and impact response; the actual vibration and temperature rise of a lubricated protective bearing are attenuated by the film and by the squeeze-film damping, and this should be taken into account when the

experimental results are extrapolated to service conditions. Second, the damage process itself changes the lubrication state: the wear and the roughening of the groove surface increase the roughness, reduce the effective film thickness and thus accelerate asperity contact and damage, which forms a positive feedback loop, and the ageing of the grease acts in the same direction [183]. Both effects should be included in the meso-scale model proposed in Section 6.

5.3. Comparison of the Reviewed Models and Limitations of the Present Work

Tables 1–3 summarize the models and methods reviewed in Sections 2–4 and list, for each of them, the key assumptions and the main limitations, so that the models can be compared directly instead of being described one after another. Several gaps emerge from this comparison. (i) Most of the quasi-static and dynamic models assume either an ideal smooth surface or a simple deterministic defect geometry (a rectangular notch or a cylindrical dent), so that the multi-scale non-smoothness of a real worn surface is not represented [47,86]. (ii) The damage is usually introduced as an excitation function (a pulse or a time-varying displacement), which is a reasonable engineering simplification but discards the geometric and material information of the damage [91,97,104]. (iii) The contact is generally treated as dry and elastic, and the lubricant film, its damping and its water content are rarely included, although Section 5.2 shows that they change both the film thickness and the vibration level [67,171]. (iv) The trade-off between accuracy and computational cost is not discussed systematically, even though the finite-element, discrete-element and discrete-dislocation methods are applied at very different scales [116]. (v) In most of the studies the damage is treated as a static geometry, whereas the wear of a local functional groove evolves with time and, as shown in Section 1, continuously changes the contact radius and the orbital velocity of the rolling elements [155].

The limitations of the studies reviewed here, and of the experimental work that underlies them, must also be stated explicitly. First, the experiments were performed under dry friction. In a lubricated contact the hydrodynamic and squeeze-film effects discussed in Section 5.2 suppress the oscillations and the vibration of the rolling elements and thus change both the amplitude and the spectrum of the measured signals; the conclusions drawn from the dry-friction tests are therefore conservative rather than generally valid. Second, the artificial rectangular defects produced by electrical discharge machining reproduce the size but not the morphology of real tribological damage. In service, the edges of the damage are progressively rounded and smoothed by plastic deformation: the effective edge angle decreases, the entry and exit slopes along which the rolling elements pass become gentler, the shock pulses are weakened and the vibration energy is transferred to lower harmonics. Idealized rectangular defects therefore overestimate the high-frequency impact components while underestimating the low-frequency modulation of the vibration signal. The decisive influence of the defect morphology on the vibration response has been confirmed by comparing dent and bump faults of different geometries [184], by modelling the spall size and the corresponding strain and vibration signature [185] and by analysing the friction-induced stick–slip vibration of rough contacts [186]. In future experimental work these features should be reproduced either by preparing defects with rounded or worn edges, or by measuring the three-dimensional morphology of the damage before the vibration test and by using it as the input of the model.

6. Future Research Directions

In order to clearly separate the authors' proposal from the overview given in Sections 2–4, the future and partially ongoing research work is summarized separately in this section.

(1) A multi-scale damage-evolution framework for local functional grooves should be established, in which the meso-scale degradation of the groove surface is described by the bond-fracture model of the discrete element method and is fed back to the macroscopic dynamic model of the bearing. In this way the wear of the groove, the variation in the contact radius and the change in the self-dispersing behaviour of the rolling elements can be predicted simultaneously instead of being treated as independent problems.

(2) The idealized rectangular defect should be replaced by a parametric real-damage morphology in which the edge radius, the edge angle, the depth and the three-dimensional spalling profile are explicitly described, and the influence of the plastic-deformation-induced rounding of the groove edges on the shock pulse and on the vibration spectrum should be quantified experimentally and numerically.

(3) The contact and dynamic models should be extended from dry friction to lubricated conditions by introducing the elastohydrodynamic film thickness, the traction and the squeeze-film damping between the rolling elements and the groove surface, and by treating the type of lubricant (oil or grease), its ageing state and its water content as explicit parameters.

(4) The geometry of the local functional groove should be optimized as a surface-texture design problem: the depth, width, edge radius, spacing and areal density of the grooves should be optimized with respect to both the self-dispersing effect and the damage tolerance, instead of being selected empirically [163].

(5) An instrumented protective-bearing test rig combining high-speed photography, vibration, temperature and acoustic-emission measurements should be developed, and the experiments should be carried out over a matrix of rotational speeds and loads with a sufficient number of repetitions, so that the scatter and the margin of error of the measured self-dispersing behaviour can be quantified; the same rig should be used to validate the lubricated and the water-contaminated conditions.

(6) Finally, the meso-scale damage model should be integrated into a digital twin of the protective bearing, so that the wear state of the local functional grooves can be estimated from the measured vibration and temperature signals and the remaining life of the protective bearing can be predicted, providing a basis for the timely replacement of the protective bearings of magnetic-bearing systems.

7. Conclusions

This review has been organized so that the overview of the state of the art (Sections 2–4), the critical discussion (Section 5) and the authors' proposal for future research (Section 6) are clearly separated. The main conclusions of the overview are as follows.

In summary, to explore the motion mechanism and non-smooth contact behavior of rolling bearings in practical work, scholars at home and abroad have simulated the actual working conditions of bearings through established lumped parameter models, quasi-static models, quasi-dynamic models, and dynamic models. They have studied phenomena such as cage slippage, cage impact, and rolling element slippage. However, the constraint conditions of current bearing theoretical models are usually determined by the coupling relationship between various components, ignoring the changes in the contact model between the rolling elements and various bearing components caused by the time-varying actual working posture of the rolling elements. Therefore, based on the research of the aforementioned scholars, considering the non-smooth contact state of the local functional groove surface under multiple postures such as orbital revolution, rotation, spin, slippage, and fretting sliding, the established bearing theoretical model can be made more accurate.

The damage to rolling bearings is caused by a combination of factors and is influenced by load, speed, lubrication, and environmental conditions. Scholars generally adopt two

approaches to study the bearing surface: one is to determine the extent of bearing damage by establishing vibration excitation, and the other is to predict the fatigue life of the bearing by constructing the geometric morphology of the damaged surface. Existing research on bearings mostly focuses on macroscopic stress, contact deformation, or the material itself, but research from a single perspective and scale cannot truly characterize the operating conditions of bearings during operation. Therefore, it is necessary to conduct research on multi-scale and multi-factor damage mechanisms.

The discrete element method has been widely applied in the field of mechanical wear. Scholars both domestically and internationally utilize the contact model within the discrete element method to simulate the interaction between particles and geometric bodies. The connection model discretizes macroscopic components into mesoscopic particle models, predicting macroscopic wear through the number of broken connection bonds. Although scholars have applied the discrete element method to bearing wear, there is limited theoretical research on the changes in particle geometry size due to changes in the friction coefficient caused by raceway damage after discretization. Additionally, research on the mapping relationship between the force transfer law between particles and the behavior of connection bond fracture is not sufficiently in-depth.

For the cageless ball bearing with local functional grooves that is used as the protective bearing of a magnetic bearing, however, the mapping relationship between the meso-scale damage of the groove surface and the macroscopic discrete performance of the rolling elements has not yet been established. The clarification of the non-smooth nature of the groove surface (Section 5.1), the explicit consideration of the lubricant and of its water content (Section 5.2), the comparative analysis of the reviewed models (Section 5.3, Tables 1–3) and the multi-scale framework proposed in Section 6 therefore constitute both the main contribution of this review and the direction of the authors' ongoing work.

Author Contributions: Conceptualization, Y.Z. and E.Z.; methodology, E.Z.; software, E.Z.; validation, E.Z. and Y.W.; formal analysis, J.Z.; investigation, Y.Z.; resources, Y.Z.; data curation, E.Z.; writing—original draft preparation, E.Z.; writing—review and editing, E.Z.; visualization, E.Z.; supervision, Y.Z. All authors have read and agreed to the published version of the manuscript.

Funding: This work was financially supported by the Jilin Provincial Department of Education Scientific Research Project (JJKH20251825KJ), 2026 Annual Planning Project of the China Vocational Education Society (ZJS2026YB112) and Jilin Tiedao University Doctoral Research Start-up Fund.

Data Availability Statement: The original contributions presented in this study are included in the article. Further inquiries can be directed to the corresponding author.

Conflicts of Interest: Authors Jingwei Zhang and Enwen Zhou are employed by the company Goertek Inc. Postdoctoral Research Station, Goertek Co., Ltd. The remaining authors declare that the research was conducted in the absence of any commercial or financial relationships that could be construed as a potential conflict of interest.

References

1. Vehviläinen, M.; Rahkola, P.; Keränen, J.; Halme, J.; Sopanen, J.; Liukkonen, O.; Holopainen, A.; Tammi, K.; Belahcen, A. Adapting Geometry-Based Polygonal Contacts for Simulating Faulty Rolling Bearing Dynamics. *Mech. Mach. Theory* **2024**, *192*, 105552. [CrossRef]
2. Guo, D.; Lu, Y. Overview of Extreme Manufacturing. *Int. J. Extrem. Manuf.* **2019**, *1*, 020201. [CrossRef]
3. Salunkhe, V.G.; Desavale, R.G.; Kumbhar, S.G. Vibration Analysis of Deep Groove Ball Bearing Using Finite Element Analysis and Dimension Analysis. *J. Tribol.* **2022**, *144*, 081202. [CrossRef]
4. Liu, Y.; Chen, Z.; Tang, L.; Zhai, W. Skidding Dynamic Performance of Rolling Bearing with Cage Flexibility under Accelerating Conditions. *Mech. Syst. Signal Process.* **2021**, *150*, 107257. [CrossRef]
5. Rubini, R.; Meneghetti, U. Application of the Envelope and Wavelet Transform Analyses for the Diagnosis of Incipient Faults in Ball Bearings. *Mech. Syst. Signal Process.* **2001**, *15*, 287–302. [CrossRef]

6. Zhang, P.; Du, Y.; Habetler, T.G.; Lu, B. A Survey of Condition Monitoring and Protection Methods for Medium-Voltage Induction Motors. *IEEE Trans. Ind. Appl.* **2010**, *47*, 34–46. [CrossRef]
7. Tan, D.Q.; Li, R.; He, Q.; Yang, X.Q.; Zhou, C.Q.; Mo, J.L. Failure Analysis of the Joint Bearing of the Main Rotor of the Robinson R44 Helicopter: A Case Study. *Wear* **2021**, *477*, 203862. [CrossRef]
8. Cong, F.; Chen, J.; Dong, G.; Pecht, M. Vibration Model of Rolling Element Bearings in a Rotor-Bearing System for Fault Diagnosis. *J. Sound Vib.* **2013**, *332*, 2081–2097. [CrossRef]
9. Vehviläinen, M.; Tahkola, M.; Keränen, J.; El Bouharrouti, N.; Rahkola, P.; Halme, J.; Pippuri-Mäkeläinen, J.; Belahcen, A. 3D Multibody Simulation of Realistic Rolling Bearing Defects for Fault Classifier Development. In *Proceedings of the 2024 International Conference on Electrical Machines (ICEM), Torino, Italy*; IEEE: New York, NY, USA, 2024; pp. 1–7. [CrossRef]
10. Shen, Q.; Zhou, Z.; Li, S.; Liao, X.; Wang, T.; He, X.; Zhang, J. Design and Analysis of the High-Speed Permanent Magnet Motors: A Review on the State of the Art. *Machines* **2022**, *10*, 549. [CrossRef]
11. Pang, X.; Zhu, D.; Qiu, M.; Wang, D.; Wang, X. Eccentric Rotor Drop Dynamics Study of Vertical Maglev Bearing System. *Lubricants* **2023**, *11*, 246. [CrossRef]
12. Sun, B.; Sheng, Z.; Song, P.; Sun, H.; Wang, F.; Sun, X.; Liu, J. State-of-the-Art Detection and Diagnosis Methods for Rolling Bearing Defects: A Comprehensive Review. *Appl. Sci.* **2025**, *15*, 1001. [CrossRef]
13. Li, Y.J.; Tao, C.H.; Zhang, W.F.; Jiang, T. Fracture Analysis on Cage Rivets of a Cylindrical Roller Bearing. *Eng. Fail. Anal.* **2008**, *15*, 796–801. [CrossRef]
14. Syla, S.; Brill, K.M.; Paulus, S.; Graf, S.; Koch, O. A Detailed Multibody Simulation Model for Ball Bearings to Predict Friction and Electrical Capacitance. *Lubricants* **2026**, *14*, 154. [CrossRef]
15. Zhao, Y.; Yang, G.; Keogh, P.S.; Zhao, L. Dynamic Analysis for the Rotor Drop Process and Its Application to a Vertically Levitated Rotor/Active Magnetic Bearing System. *J. Tribol.* **2017**, *139*, 041701. [CrossRef]
16. Qin, S. Design and Dynamics Research of Variable Speedcurved Surface of Bearing Without Cage. Master's Thesis, Harbin University of Science and Technology, Harbin, China, 2020. [CrossRef]
17. Wang, Q.Y. Research on Dynamic Characteristics andAutomatic Discrete Dynamics of theRolling Element of Cageless Ball Bearings. Ph.D. Dissertation, Harbin University of Science and Technology, Harbin, China, 2023. [CrossRef]
18. Kawamura, H.; Touma, K. Motion of Unbalanced Balls in High-Speed Angular Contact Ball Bearings. *J. Tribol.* **1990**, *112*, 105–110. [CrossRef]
19. Zhan, L.; Li, Z.; Zhuo, S.; Wang, X.; Liu, J. Study on Cage Slip for Rolling Bearing Under Speed Variation Conditions. *Struct. Health Monit.* **2023**, *22*, 966–977. [CrossRef]
20. Liu, Y.; Chen, Z.; Zhai, W.; Wang, K. Investigation on Skidding Behavior of a Lubricated Rolling Bearing with Fluid-Solid-Heat Coupling Effect. *Mech. Syst. Signal Process.* **2024**, *206*, 110922. [CrossRef]
21. Liu, Y.; Chen, Z.; Li, Y.; Zhai, W.; Wang, K. Dynamic Investigation and Alleviative Measures for the Skidding Phenomenon of Lubricated Rolling Bearing under Light Load. *Mech. Syst. Signal Process.* **2023**, *184*, 109685. [CrossRef]
22. Jones, A.B. Ball Motion and Sliding Friction in Ball Bearings. *J. Basic Eng.* **1959**, *81*, 1–12. [CrossRef]
23. Walters, C.T. The Dynamics of Ball Bearings. *J. Tribol.* **1971**, *93*, 1–10. [CrossRef]
24. Gupta, P.K. Transient Ball Motion and Skid in Ball Bearings. *J. Tribol.* **1975**, *97*, 261–269. [CrossRef]
25. Li, Y.; Li, Z.; He, D.; Wang, X. Effect of Clearance on the Dynamic Characteristics of High-Speed Rolling Bearings with Multiple Defects. *Mech. Syst. Signal Process.* **2023**, *200*, 110512. [CrossRef]
26. Hirano, F. Motion of a Ball in Angular-Contact Ball Bearing. *Asle Trans.* **1965**, *8*, 425–434. [CrossRef]
27. Zhang, J.; Zhou, E.; Wang, Y.; Lv, Q.; Zhang, Y. Experimental Study on the Non-Smooth Behavior of Cage-Less Ball Bearings with Localized Functional Grooves. *Machines* **2026**, *14*, 419. [CrossRef]
28. Harris, T.A. An Analytical Method to Predict Skidding in Thrust-Loaded, Angular-Contact Ball Bearings. *J. Lubr. Technol.* **1971**, *93*, 17–23. [CrossRef]
29. Liao, N.T.; Lin, J.F. Ball Bearing Skidding under Radial and Axial Loads. *Mech. Mach. Theory* **2002**, *37*, 91–113. [CrossRef]
30. Xiong, Q.; Tang, J.; Ding, T.; Zhang, W. Dynamic Modeling and Vibration Response Analysis of Rolling Bearings with Composite Faults Considering the Influence of Elastohydrodynamic Lubrication. *Shock Vib.* **2024**, *2024*, 1057592. [CrossRef]
31. Guo, S.; Wang, W.; Tang, R.; Liang, H.; Zhang, H. The Effect of External Load on Multi-Point Contact Transitions of Three-Point Angular Contact Ball Bearing. *Mech. Mach. Theory* **2026**, *220*, 106368. [CrossRef]
32. Sharma, A.; Sadeghi, F. Effects of Fretting Wear on Rolling Contact Fatigue. *Tribol. Int.* **2024**, *192*, 109204. [CrossRef]
33. Sheng, X.; Lu, X.; Zhang, J.; Wang, Y. An Analytical Solution to Temperature Field Distribution in a Thick Rod Subjected to Periodic-Motion Heat Sources and Application in Ball Screws. *Eng. Optim.* **2021**, *53*, 2144–2163. [CrossRef]
34. Wang, L.; Hu, C.; Hu, L.; Liu, F.; Tang, H. An Investigation on the Mechanical Characteristics of Railway Locomotive Axle Box Bearings with Sensor-Embedded Slots. *Machines* **2025**, *13*, 358. [CrossRef]
35. Singh, S.; Howard, C.Q.; Hansen, C.H. An Extensive Review of Vibration Modelling of Rolling Element Bearings with Localised and Extended Defects. *J. Sound Vib.* **2015**, *357*, 300–330. [CrossRef]

36. Sun, J.; Guo, H.; Guo, X.; Zhang, Y.; Liu, Y. The Simulation Analysis and Experimental Study on the Temperature Field of Four Row Rolling Bearings of Rolling Mill under Non-Uniform Load Conditions. *Sensors* **2024**, *24*, 914. [CrossRef]
37. Liu, Y.; Zhu, M.; Lu, X.; Zhang, H.; Chen, L. A Review of Cross-Scale Theoretical Contact Models for Bolted Joints Interfaces. *Coatings* **2024**, *14*, 539. [CrossRef]
38. Meguid, S.A.; Czekanski, A. Advances in Computational Contact Mechanics. *Int. J. Mech. Mater. Des.* **2008**, *4*, 419–443. [CrossRef]
39. Lundberg, G.; Arvid, P. Dynamic Capacity of Rolling Bearings. *J. Appl. Mech.* **1949**, *16*, 165–172. [CrossRef]
40. Sinha, R.; Sahoo, V.; Paswan, M. Radial Load Distribution by Balls in a Ball Bearing with Variable Clearance. *Mech. Based Des. Struct. Mach.* **2023**, *51*, 3538–3563. [CrossRef]
41. Sinha, R.; Sahoo, V.; Paswan, M.; Routh, B. An Analytical Method of Axial Load Distribution of Deep Groove Variable Clearance Radial Ball Bearings. *Mech. Based Des. Struct. Mach.* **2024**, *52*, 1669–1685. [CrossRef]
42. Neisi, N.; Sikanen, E.; Heikkinen, J.E.; Sopanen, J. Effect of Off-Sized Balls on Contact Stresses in a Touchdown Bearing. *Tribol. Int.* **2018**, *120*, 340–349. [CrossRef]
43. Gao, S.; Meng, G. Unstable Islands and Bifurcation Analysis in a Spindle Milling System Supported by Ball Bearings. *Proc. Inst. Mech. Eng. Part K J. Multi-Body Dyn.* **2011**, *225*, 235–251. [CrossRef]
44. Zhang, Y.; Fang, B.; Kong, L.; Hou, L.; Li, Y. Effect of the Ring Misalignment on the Service Characteristics of Ball Bearing and Rotor System. *Mech. Mach. Theory* **2020**, *151*, 103889. [CrossRef]
45. Gao, S.; Nong, S.; Meng, G.; Fang, T. Frequency Response Curves of a Spindle Bearings System with Non-Linear and Non-Smooth Terms. *Proc. Inst. Mech. Eng. Part K J. Multi-Body Dyn.* **2013**, *227*, 61–75. [CrossRef]
46. Liu, Y.; Li, X.; Liu, H.; Wang, Y. Time-Varying Meshing Stiffness Model of the Idler Ring Bearing in Planetary Gear Train. *Mech. Mach. Theory* **2026**, *219*, 106322. [CrossRef]
47. Xiao, L.; Rosen, B.G.; Amini, N.; Almqvist, A. A Study on the Effect of Surface Topography on Rough Friction in Roller Contact. *Wear* **2003**, *254*, 1162–1169. [CrossRef]
48. Zhang, Z.; Xu, X.; Gong, W.; Chen, Z. Efficient Federated Convolutional Neural Network with Information Fusion for Rolling Bearing Fault Diagnosis. *Control Eng. Pract.* **2021**, *116*, 104913. [CrossRef]
49. Tu, W.; Wang, H.; Liu, C.; Zhang, Y. Influence of Temperature on Dynamic Contact Characteristics of Oil-Jet Lubricated Rolling Bearings. *Proc. Inst. Mech. Eng. Part K J. Multibody Dyn.* **2024**, *238*, 167–181. [CrossRef]
50. Zhou, E.; Zhang, J.; Fan, L.; Qi, H.; Zhang, Y.; Zhang, H. A Study on the Vibration Characteristics of Cage-Less Ball Bearings Following Local Damage to the Grooves. *Lubricants* **2026**, *14*, 248. [CrossRef]
51. Zhang, C.; Qin, F.; Zhao, W.; Li, J. Research on Rolling Bearing Fault Diagnosis Based on Digital Twin Data and Improved ConvNext. *Sensors* **2023**, *23*, 5334. [CrossRef]
52. Zhao, W.; Zhang, C.; Fan, B.; Liu, S. Research on Rolling Bearing Virtual-Real Fusion Life Prediction with Digital Twin. *Mech. Syst. Signal Process.* **2023**, *198*, 110434. [CrossRef]
53. Liu, C.; He, D.; Wei, Z.; Zhong, H.; Wu, J. Personalized Fault Diagnosis of Rolling Bearings in Trains Based on Digital Twin. *Meas. Sci. Technol.* **2023**, *34*, 125131. [CrossRef]
54. Farah, S.O.; Guessasma, M.; Bellenger, E. Digital Twin by DEM for Ball Bearing Operating under EHD Conditions. *Mech. Ind.* **2020**, *21*, 506. [CrossRef]
55. Gupta, P.K. *Advanced Dynamics of Rolling Elements*; Springer: New York, NY, USA, 1984. [CrossRef]
56. Gupta, P.K. Dynamics of Rolling-Element Bearings—Part IV: Ball Bearing Results. *J. Tribol.* **1979**, *101*, 319–326. [CrossRef]
57. Meeks, C.R.; Ng, K.O. The Dynamics of Ball Separators in Ball Bearings—Part I: Analysis. *Asle Trans.* **1985**, *28*, 277–287. [CrossRef]
58. Wagner, C.; Krinner, A.; Thümmel, T.; Rixen, D. Full Dynamic Ball Bearing Model with Elastic Outer Ring for High Speed Applications. *Lubricants* **2017**, *5*, 17. [CrossRef]
59. Houpert, L. Cagedyn: A Contribution to Roller Bearing Dynamic Calculations Part I: Basic Tribology Concepts. *Tribol. Trans.* **2010**, *53*, 1–9. [CrossRef]
60. Beswick, J.; Voskamp, A.; van den Sanden, J. Bearing Material/Treatment Developments at the SKF Engineering and Research Centre. *Creat. Use Bear. Steels* **1993**, *1195*, 222. [CrossRef]
61. Ma, W.; Ma, S.; Zou, Z.; Wang, Y.; Liu, J. Literature Review on Fault Mechanism Analysis and Diagnosis Methods for Main Pump Systems. *Machines* **2025**, *13*, 1000. [CrossRef]
62. Cui, L.; Su, Y. Contact Fatigue Life Prediction of Rolling Bearing Considering Machined Surface Integrity. *Ind. Lubr. Tribol.* **2022**, *74*, 73–80. [CrossRef]
63. Su, B.; Lu, C.; Li, C. Current Status of Research on Hybrid Ceramic Ball Bearings. *Machines* **2024**, *12*, 510. [CrossRef]
64. Yang, F.; Guo, Q.; Chen, L.; Zhang, H.; Zhou, Y. Rolling Bearing Digital Twin Model Oriented Toward Rotational Accuracy Prediction. *Meas. Sci. Technol.* **2026**, *37*, 045013. [CrossRef]
65. Ozsarac, U.; Findik, F.; Durman, M. The Wear Behaviour Investigation of Sliding Bearings with a Designed Testing Machine. *Mater. Des.* **2007**, *28*, 345–350. [CrossRef]

66. Kang, S.Q.; Yang, J.W.; Wang, Y.J.; Wang, Q.Y.; Xie, J.B. Fault diagnosis method of rolling bearings under different working conditions based on federated multi-representation domain adaptation. *Chin. J. Sci. Instrum.* **2023**, *44*, 165–176. [CrossRef]
67. Bal, H.; Ateş, K.; Karaçay, T.; Aktürk, N. Effect of Preload on the Vibrations of EHL Angular Contact Ball Bearings: Theoretical and Experimental Results. *Lubricants* **2022**, *10*, 46. [CrossRef]
68. Madiedo, J.M.; Franco, J.M.; Valencia, C.; Sánchez, M. Modeling of the Non-Linear Rheological Behavior of a Lubricating Grease at Low-Shear Rates. *J. Tribol.* **2000**, *122*, 590–596. [CrossRef]
69. Chen, C.; Wang, X.; Shen, Y.; Liu, Z. Experimental Investigation for Vibration Reduction of Surface-Textured Journal Bearings. *Ind. Lubr. Tribol.* **2019**, *71*, 232–241. [CrossRef]
70. Lei, J.; Zhou, R.; Chen, H.; Gao, Y.; Lai, G. Experimental Investigation of Effects of Ship Propulsion Shafting Alignment on Shafting Whirling and Bearing Vibrations. *J. Mar. Sci. Technol.* **2022**, *27*, 151–162. [CrossRef]
71. Wang, Y.; Shiyuan, E. Design and Research of Bearing Reliability Test Bed Based on Multi-Dimensional Vibration Loading. *J. Phys. Conf. Ser.* **2021**, *2101*, 012045. [CrossRef]
72. Wei, H.; Cai, G.; Liu, Z.; Wu, Z. A Fusion Non-Convex Group Sparsity Difference Method and Its Application in Rolling Bearing Fault Diagnosis. *Meas. Sci. Technol.* **2024**, *35*, 025123. [CrossRef]
73. Xu, C.; Wu, T.; Yang, H.; Liu, Y. Study on Vibration Mechanism Induced by Skidding in Pure Rolling Contact. *Tribol. Int.* **2021**, *154*, 106669. [CrossRef]
74. McColl, I.R.; Ding, J.; Leen, S.B. Finite Element Simulation and Experimental Validation of Fretting Wear. *Wear* **2004**, *256*, 1114–1127. [CrossRef]
75. Song, L.; Wang, H.; Chen, P. Vibration-Based Intelligent Fault Diagnosis for Roller Bearings in Low-Speed Rotating Machinery. *IEEE Trans. Instrum. Meas.* **2018**, *67*, 1887–1899. [CrossRef]
76. Li, Y.; Chen, X.; Zhang, P.; Wang, Z. Dynamics Modeling and Modal Experimental Study of High Speed Motorized Spindle. *J. Mech. Sci. Technol.* **2017**, *31*, 1049–1056. [CrossRef]
77. Li, S.H.; Wu, Y.H.; Zhang, L.X. Development and Experimental Investigation of a High Speed Grinding Spindle Equipped with Fully-Ceramic Bearings and Ceramic Shaft. *Adv. Mater. Res.* **2011**, *156*, 1366–1371. [CrossRef]
78. Townsend, D.P.; Allen, C.W.; Zaretsky, E.V. *Friction Losses in a Lubricated Thrust-Loaded Cageless Angular-Contact Bearing*; NASA Technical Report; NASA: Washington, DC, USA, 1973.
79. Zhil'nikov, E.; Balyakin, V.; Lavrin, A. A Method for Calculating the Frictional Moment in Cageless Bearings. *J. Frict. Wear* **2018**, *39*, 400–404. [CrossRef]
80. Gao, F.W.; Deng, S.E.; Zhu, K.M.; Li, G.B.; Liao, J.X.; Liu, J.X. Non-contact Instrument for Starting Friction Torque of Bearings. *Bearing* **2009**, *4*, 39–42. [CrossRef]
81. Xiong, W.; Zheng, G.; Zhang, H.; Li, J.; Liu, S. Load Characteristics and Friction Torque Analysis of Triple-Row Wheel Hub Bearings. *Lubricants* **2026**, *14*, 45. [CrossRef]
82. Zhao, Y.; Wu, C. Numerical Simulation to Research the Collision and Skidding of Rolling Elements for Cageless Bearings. *Ind. Lubr. Tribol.* **2022**, *74*, 1101–1109. [CrossRef]
83. Gao, X.; Zhang, C.Y. A Study on Measuring Method for 3D Motion of Balls in High-Speed Ball Bearings. *Adv. Mater. Res.* **2011**, *199*, 449–455. [CrossRef]
84. Gentle, C.; Boness, R. Prediction of Ball Motion in High-Speed Thrust-Loaded Ball Bearings. *J. Lubr. Technol.* **1976**, *98*, 463–471. [CrossRef]
85. Yun, X.; Han, Q.; Wen, B.; Hao, X. Dynamic Stiffness and Vibration Analysis Model of Angular Contact Ball Bearing Considering Vibration and Friction State Variation. *J. Vibroeng.* **2022**, *24*, 221–255. [CrossRef]
86. Adamczak, S.; Zmarzły, P. Research of the Influence of the 2D and 3D Surface Roughness Parameters of Bearing Raceways on the Vibration Level. *J. Phys. Conf. Ser.* **2019**, *1183*, 012001. [CrossRef]
87. Ebert, F.J. Fundamentals of Design and Technology of Rolling Element Bearings. *Chin. J. Aeronaut.* **2010**, *23*, 123–136. [CrossRef]
88. Moundekar, N.D.; Deshmukh, B.D. Study of Failure Modes of Rolling Bearings: A Review. *Int. J. Mod. Eng. Res.* **2014**, *4*, 139–143.
89. El-Thalji, I.; Jantunen, E. Fault Analysis of the Wear Fault Development in Rolling Bearings. *Eng. Fail. Anal.* **2015**, *57*, 470–482. [CrossRef]
90. Li, N.; Li, R.; Cui, L.; Wang, H.; Zhang, Y. Fatigue Failure Mechanisms and Multi-Factor Coupled Modeling of Roller Bearings: A Review. *Int. J. Adv. Manuf. Technol.* **2026**, *143*, 6113–6143. [CrossRef]
91. Khanam, S.; Dutt, J.; Tandon, N. Impact Force Based Model for Bearing Local Fault Identification. *J. Vib. Acoust.* **2015**, *137*, 051002. [CrossRef]
92. Zhang, X.; Wu, D.; Xia, Z.; Liu, X.; Wang, R. Characteristics and Mechanism of Surface Damage of Hybrid Ceramic Ball Bearings for High-Precision Machine Tool. *Eng. Fail. Anal.* **2022**, *142*, 106784. [CrossRef]
93. Guan, Z.Z.; Zheng, H.Q.; Yang, Y.T.; Chen, X.H. Fault diagnosis of bearing based on nonlinear time series of geometrical invariants. *J. Vib. Shock* **2009**, *28*, 130–133+209. [CrossRef]

94. Chen, G. Nonlinear Dynamics of Unbalance-looseness Coupling Faults of Rotor-ball Bearing-stator Coupling System. *J. Mech. Eng.* **2008**, *44*, 82–88. [CrossRef]
95. Martin, G.; Becker, F.M.; Kirchner, E. A Novel Method for Diagnosing Rolling Bearing Surface Damage by Electric Impedance Analysis. *Tribol. Int.* **2022**, *170*, 107503. [CrossRef]
96. Chen, L.; Fang, M.; Qiu, M.; Zhang, H.; Li, J. Analyzing Vibration Mechanism of Angular Contact Ball Bearing with Compound Faults on Inner and Outer Rings. *Shock Vib.* **2021**, *2021*, 9951110. [CrossRef]
97. Wang, H.; Wang, P.; Wang, S.; Liu, Y.; Zhao, L. Rolling Bearing Fault Diagnosis Method Based on Dynamic Simulated Model from Source Domain to Target Domain with Improved Alternating Transfer Learning. *Nonlinear Dyn.* **2025**, *113*, 4485–4510. [CrossRef]
98. Jamadar, I.M.; Suresha, B.; Samal, P.K.; Bellary, S.A.I. Dimensional Amplitude Response Analysis of Vibrations Produced by Defects in Rolling Contact Bearings. *Sound Vib.* **2022**, *56*, 27. [CrossRef]
99. Lu, Y. Dynamic Modeling and Simulation of Spalling Fault of Deep Groove Ball Bearing. *J. Hubei Univ. Technol.* **2023**, *38*, 34–38+54.
100. McFadden, P.D.; Smith, J.D. Model for the Vibration Produced by a Single Point Defect in a Rolling Element Bearing. *J. Sound Vib.* **1984**, *96*, 69–82. [CrossRef]
101. Fan, J.; Cui, W.; Han, Q. Vibration Signal Modeling of a Localized Defective Rolling Bearing under Unbalanced Force Excitations. *J. Vibroeng.* **2017**, *19*, 5009–5019. [CrossRef]
102. Behzad, M.; Bastami, A.R.; Mba, D. A New Model for Estimating Vibrations Generated in the Defective Rolling Element Bearings. *J. Vib. Acoust.* **2011**, *133*, 041011. [CrossRef]
103. Liu, J.; Shao, Y.; Zhu, W. A New Model for the Relationship between Vibration Characteristics Caused by the Time-Varying Contact Stiffness of a Deep Groove Ball Bearing and Defect Sizes. *J. Tribol.* **2015**, *137*, 031101. [CrossRef]
104. Jiang, Y.C.; Huang, W.T.; Luo, J.N.; Wang, W.J. An Improved Dynamic Model of Defective Bearings Considering the Three-Dimensional Geometric Relationship between the Rolling Element and Defect Area. *Mech. Syst. Signal Process.* **2019**, *129*, 694–716. [CrossRef]
105. Ghezzi, I.; Komba, E.W.H.; Tonazzi, D.; Bouscharain, N.; Le Jeune, G.; Coudert, J.B.; Massi, F. Damage Evolution and Contact Surfaces Analysis of High-Loaded Oscillating Hybrid Bearings. *Wear* **2018**, *406–407*, 1–12. [CrossRef]
106. Lai, J.; Stadler, K. Investigation on the Mechanisms of White Etching Crack (WEC) Formation in Rolling Contact Fatigue and Identification of a Root Cause for Bearing Premature Failure. *Wear* **2016**, *364–365*, 244–256. [CrossRef]
107. Chiu, Y.P.; Tallian, T.E.; McCool, J.I. An Engineering Model of Spalling Fatigue Failure in Rolling Contact: I. The Subsurface Model. *Wear* **1971**, *17*, 433–446. [CrossRef]
108. Lian, Q.L.; Zhu, H.T.; Deng, G.Y.; Wang, X.M.; Li, H.J.; Wang, X.; Liu, Z.M. Evolution of Thermally Induced White Etching Layer at Rail Surface During Multiple Wheel/Train Passages. *Int. J. Fatigue* **2022**, *159*, 106799. [CrossRef]
109. Yan, H.; Wei, P.T.; Su, L.H.; Liu, H.J.; Wei, D.; Zhang, X.H.; Deng, G.Y. Rolling-Sliding Contact Fatigue Failure and Associated Evolutions of Microstructure, Crystallographic Orientation and Residual Stress of AISI 9310 Gear Steel. *Int. J. Fatigue* **2023**, *170*, 107511. [CrossRef]
110. Ren, Z.; Li, B.; Zhou, Q. Rolling Contact Fatigue Crack Propagation on Contact Surface and Subsurface in Mixed Mode I+II+III Fracture. *Wear* **2022**, *506–507*, 204459. [CrossRef]
111. Tallian, T.E. Simplified Contact Fatigue Life Prediction Model—Part I: Review of Published Models. *J. Tribol.* **1992**, *114*, 207–213. [CrossRef]
112. Tallian, T.E. Simplified Contact Fatigue Life Prediction Model—Part II: New Model. *J. Tribol.* **1992**, *114*, 214–220. [CrossRef]
113. Voskamp, A.P. Microstructural Stability and Bearing Performance. In *Bearing Steel Technology*; ASTM International: West Conshohocken, PA, USA, 2002.
114. Littmann, W.E.; Widner, R.L. Propagation of Contact Fatigue from Surface and Subsurface Origins. *J. Basic Eng.* **1966**, *88*, 624–636. [CrossRef]
115. Smith, J.O.; Liu, C.K. Stresses Due to Tangential and Normal Loads on an Elastic Solid with Application to Some Contact Stress Problems. *J. Appl. Mech.* **1953**, *20*, 157–166. [CrossRef]
116. Vakis, A.I.; Yastrebov, V.A.; Scheibert, J.; Nicola, L.; Dini, D.; Minfray, C.; Almqvist, A.; Paggi, M.; Lee, S.; Limbert, G.; et al. Modeling and Simulation in Tribology across Scales: An Overview. *Tribol. Int.* **2018**, *125*, 169–199. [CrossRef]
117. Bemporad, A.; Paggi, M. Optimization Algorithms for the Solution of the Frictionless Normal Contact between Rough Surfaces. *Int. J. Solids Struct.* **2015**, *69–70*, 94–105. [CrossRef]
118. Li, H.X.; Jin, X.H.; Ye, P.; Gui, X.C.; Hou, W.F. Research of Time-varying Mesh Characteristics of Cycloid Internal Gear Pair with High Contact Ratio Based on Finite Element Method. *J. Mech. Eng.* **2021**, *57*, 206–219. [CrossRef]
119. Deng, Y.B. Analytical Theory and Finite Element Analysis for Consolidation of Soft Soils by Vertical Drains. Ph.D. Dissertation, Zhejiang University, Hangzhou, China, 2013.
120. Spence, D.A. The Hertz Contact Problem with Finite Friction. *J. Elast.* **1975**, *5*, 297–319. [CrossRef]
121. Sahlin, F.; Larsson, R.; Almqvist, A.; Lundström, T.S. A Mixed Lubrication Model Incorporating Measured Surface Topography. Part 1: Theory of Flow Factors. *Proc. Inst. Mech. Eng. Part J J. Eng. Tribol.* **2010**, *224*, 335–351. [CrossRef]

122. Sahlin, F.; Larsson, R.; Marklund, P.; Almqvist, A.; Lundström, T.S. A Mixed Lubrication Model Incorporating Measured Surface Topography. Part 2: Roughness Treatment, Model Validation, and Simulation. *Proc. Inst. Mech. Eng. Part J J. Eng. Tribol.* **2010**, *224*, 353–365. [CrossRef]
123. Wang, J. Mechanism Study on the Influences ofSurface Texture on the Friction andAbrasion Characteristics of Mould Surface. Ph.D. Dissertation, Chongqing University, Chongqing, China, 2017.
124. Pan, E.S.; Wang, S.Y.; Yang, W.T.; Hu, Z.W. Computer Simulation of Gearing about Load, Stress and Wear in Meshing Process. *Mech. Sci. Technol.* **2000**, *19*, 40–41. [CrossRef]
125. Van der Giessen, E.; Needleman, A. Discrete Dislocation Plasticity: A Simple Planar Model. *Model. Simul. Mater. Sci. Eng.* **1995**, *3*, 689. [CrossRef]
126. Ren, S.Y. Study on Microstructure Evolution of Nanoporous Metal Ligaments Under Basic Deformation. Master's Thesis, Xi'an University of Technology, Xi'an, China, 2023.
127. Wang, Z.; Ghoniem, N.; Swaminarayan, S.; LeSar, R. A Parallel Algorithm for 3D Dislocation Dynamics. *J. Comput. Phys.* **2006**, *219*, 608–621. [CrossRef]
128. Chi, Y.H.; Xiao, H.; Qie, L.C.; Zhang, Z.H.; Lu, K. Mechanical research of ice and snow splashing transponder based on a DEM-MFBD-CFD method. *J. Vib. Shock* **2023**, *42*, 290–297. [CrossRef]
129. Chen, M.Y. DEM Numerical Simulation study on the Remediationof Soil Contaminated with PCBs by Planetary Ballmill Based on DEM. Master's Thesis, Zhejiang University, Hangzhou, China, 2023. [CrossRef]
130. Komanduri, R.; Chandrasekaran, N.; Raff, L.M. MD Simulation of Indentation and Scratching of Single Crystal Aluminum. *Wear* **2000**, *240*, 113–143. [CrossRef]
131. Hakala, T.J.; Holmberg, K.; Laukkanen, A. Coupling Molecular Dynamics and Micromechanics for the Assessment of Friction and Damage Accumulation in Diamond-Like Carbon Thin Films under Lubricated Sliding Contacts. *Lubricants* **2021**, *9*, 30. [CrossRef]
132. Du, Y.Y. Study on the Mechanical Behavior of Granular Materials Based on Meso-Structure and Meso-Macro Homogenization Procedure. Ph.D. Dissertation, Dalian University of Technology, Dalian, China, 2017.
133. Cundall, P.A.; Strack, O.D.L. A Discrete Numerical Model for Granular Assemblies. *Géotechnique* **1979**, *29*, 47–65. [CrossRef]
134. Guessasma, M.; Machado, C. Three-Dimensional DEM Modelling of Ball Bearing with Lubrication Regime Prediction. *Lubricants* **2018**, *6*, 46. [CrossRef]
135. Lu, P. A Study of Particles Adhesion to Compliant Substrates with a Modified Sphere Contact Model. *Tribol. Lett.* **2015**, *58*, 6. [CrossRef]
136. Lu, G.; Third, J.; Müller, C. Discrete Element Models for Non-Spherical Particle Systems: From Theoretical Developments to Applications. *Chem. Eng. Sci.* **2015**, *127*, 425–465. [CrossRef]
137. Bertrand, F.; Leclaire, L.-A.; Levecque, G. DEM-Based Models for the Mixing of Granular Materials. *Chem. Eng. Sci.* **2005**, *60*, 2517–2531. [CrossRef]
138. Börzsönyi, T.; Stannarius, R. Granular Materials Composed of Shape-Anisotropic Grains. *Soft Matter* **2013**, *9*, 7401–7418. [CrossRef]
139. Acevedo, M.; Zuriguel, I.; Maza, D.; Pagonabarraga, I.; Alonso-Marroquin, F.; Hidalgo, R.C. Stress Transmission in Systems of Faceted Particles in a Silo: The Roles of Filling Rate and Particle Aspect Ratio. *Granul. Matter* **2014**, *16*, 411–420. [CrossRef]
140. Donev, A.; Torquato, S.; Stillinger, F.H. Neighbor List Collision-Driven Molecular Dynamics Simulation for Nonspherical Hard Particles. I. Algorithmic Details. *J. Comput. Phys.* **2005**, *202*, 737–764. [CrossRef]
141. Zhao, F.; van Wachem, B.G.M. A Novel Quaternion Integration Approach for Describing the Behaviour of Non-Spherical Particles. *Acta Mech.* **2013**, *224*, 3091–3109. [CrossRef]
142. Chen, Y.; Yang, P.P.; Zhou, Y.X.; Busso, E.P.; Guo, Z.Y.; Dong, L.T. A Micromechanics-Based Constitutive Model for Linear Viscoelastic Particle-Reinforced Composites. *Mech. Mater.* **2020**, *140*, 103228. [CrossRef]
143. Song, W.L.; Peng, Z.; Pang, S.Y.; Wang, N.; Niu, T.Y.; Hou, C.L. Particle-Chain Evolution and Constitutive Model of Magnetorheological Polishing Fluids Based on Hexagonal Close-Packed Structure. *Smart Mater. Struct.* **2020**, *29*, 045012. [CrossRef]
144. Mandø, M.; Rosendahl, L. On the Motion of Non-Spherical Particles at High Reynolds Number. *Powder Technol.* **2010**, *202*, 1–13. [CrossRef]
145. Yin, Z.X.; Peng, Y.X.; Li, T.Q.; Zhu, Z.C.; Yu, Z.F. Effect of the Operating Parameter and Grinding Media on the Wear Properties of Lifter in Ball Mills. *Proc. Inst. Mech. Eng. Part J J. Eng. Tribol.* **2020**, *234*, 1061–1074. [CrossRef]
146. Chen, G.; Schott, D.L.; Lodewijks, G. Sensitivity Analysis of DEM Prediction for Sliding Wear by Single Iron Ore Particle. *Eng. Comput.* **2017**, *34*, 2031–2053. [CrossRef]
147. Nguyen, T.; Willemsz, T.; Frijlink, H.; van der Voort Maarschalk, K. Numerical Study of Agglomerate Abrasion in a Tumbling Mixer. *Chem. Eng. Sci.* **2014**, *114*, 21–29. [CrossRef]
148. Luo, X.; Zhao, L.; Dong, H. Study on DEM Parameter Calibration and Wear Characteristics of Vanadium-Titanium Magnetite Pellets. *Powder Technol.* **2021**, *393*, 427–440. [CrossRef]
149. Luo, Y.; Tong, J.; Chen, R.; Tang, X.Z.; Peng, R.T. Numerical Study on the Ceramic Tool Abrasion in Machining Superalloy. *Int. J. Adv. Manuf. Technol.* **2020**, *111*, 2601–2614. [CrossRef]

150. Fang, Z.Q.; Hu, L.; Peng, S.L.; Yi, J.G.; Zhang, L.; Du, J. A DEM-Based Method for Predicting the Wear Evolution of Structural Boundary Composed of Spherical Boundary Elements. *Int. J. Numer. Methods Eng.* **2020**, *121*, 5667–5695. [CrossRef]
151. Zhang, R.; Chen, G.M.; Fan, W.F.; Li, J.Q.; Li, Y.W.; Liu, Z.B.; Chen, B. Simulation on the Wear Behavior of the Wear-Resistant Surfaces Using Discrete Element Method. *Adv. Mater. Res.* **2011**, *199–200*, 729–733. [CrossRef]
152. Zhang, R.; Yu, H.; Pang, H.; Tai, W.X. Analysis of Wear-Resistant Surface with Pangolin Scale Morphology by DEM Simulation. *Appl. Sci.* **2020**, *10*, 2896. [CrossRef]
153. Li, H.; Yin, Z.; Wang, Y. A Study on the Wear Behavior of Tin-Based Journal Bearing under Different Working Conditions. *Ind. Lubr. Tribol.* **2020**, *72*, 359–368. [CrossRef]
154. Zhang, Q.; Luo, J.; Xie, X.-Y.; Xu, J.; Ye, Z.-H. Experimental Study on the Skidding Damage of a Cylindrical Roller Bearing. *Materials* **2020**, *13*, 4075. [CrossRef]
155. Zhao, Y.L.; Jin, Y.; Pan, C.Y.; Wu, C.W.; Yuan, X.Y.; Zhou, G.; Han, W.G. Characterization of Bond Fracture in Discrete Groove Wear of Cageless Ball Bearings. *Materials* **2022**, *15*, 6711. [CrossRef]
156. Bourbatache, K.; Guessasma, M.; Bellenger, E.; Bourny, V.; Fortin, J. DEM Ball Bearing Model and Defect Diagnosis by Electrical Measurement. *Mech. Syst. Signal Process.* **2013**, *41*, 98–112. [CrossRef]
157. Wan, Y.Q.; Ma, B. Failure Mechanisms of the Rolling Element Bearing and the Condition Monitoring of the Large Particles Wear Metal. *J. Mech. Strength* **2000**, *22*, 161–163+193.
158. Guo, S.H. The DEM Research on Rotor System of Gear Meshing. Master's Thesis, Beijing Forestry University, Beijing, China, 2006.
159. Villavicencio, M.; Renouf, M.; Saulot, A.; Michel, Y.; Mahéo, Y.; Colas, G.; Filleter, T.; Berthier, Y. Self-Lubricating Composite Bearings: Effect of Fibre Length on Its Tribological Properties by DEM Modelling. *Tribol. Int.* **2017**, *113*, 362–369. [CrossRef]
160. Machado, C.; Guessasma, M.; Bellenger, E. An Improved 2D Modeling of Bearing Based on DEM for Predicting Mechanical Stresses in Dynamic. *Mech. Mach. Theory* **2017**, *113*, 53–66. [CrossRef]
161. Machado, C.; Baudon, S.; Guessasma, M.; Bourny, V.; Fortin, J.; Bouzerar, R.; Maier, P. An Original DEM Bearing Model with Electromechanical Coupling. *Int. J. Comput. Methods* **2019**, *16*, 1840006. [CrossRef]
162. Machado, C.; Guessasma, M.; Bourny, V. Electromechanical Prediction of the Regime of Lubrication in Ball Bearings Using Discrete Element Method. *Tribol. Int.* **2018**, *127*, 69–83. [CrossRef]
163. Lu, P.; Wood, R.J.K. Tribological Performance of Surface Texturing in Mechanical Applications—A Review. *Surf. Topogr. Metrol. Prop.* **2020**, *8*, 043001. [CrossRef]
164. Long, R.; Sun, Y.; Zhang, Y.; Shang, Q.; Ramteke, S.M.; Marian, M. Influence of Micro-Texture Radial Depth Variations on the Tribological and Vibration Characteristics of Rolling Bearings under Starved Lubrication. *Tribol. Int.* **2024**, *194*, 109545. [CrossRef]
165. Niu, Y.; Pang, X.; Yue, S.; Shangguan, B.; Zhang, Y. The Friction and Wear Behavior of Laser Textured Surfaces in Non-Conformal Contact under Starved Lubrication. *Wear* **2021**, *476*, 203723. [CrossRef]
166. Wu, C.; Yang, K.; Ni, J.; Lu, S.; Yao, L.; Li, X. Investigations for Vibration and Friction Torque Behaviors of Thrust Ball Bearing with Self-Driven Textured Guiding Surface. *Friction* **2023**, *11*, 894–910. [CrossRef]
167. Sun, S.; Long, R.; Jin, Z.; Zhang, Y.; Ju, Z.; Du, X. Research on the Friction and Wear Properties of Dents Textured Rolling Element Bearings under Dry Wear. *Coatings* **2022**, *12*, 684. [CrossRef]
168. Meng, Y. Is Laser Surface Texturing Good or Bad for Rolling Element Bearings? *Friction* **2021**, *9*, 1784–1786. [CrossRef]
169. Rahmani, R.; Rahnejat, H. Enhanced Performance of Optimised Partially Textured Load Bearing Surfaces. *Tribol. Int.* **2018**, *117*, 272–282. [CrossRef]
170. Long, R.; Zhao, C.; Zhang, Y.; Wang, Y.; Wang, Y. Effect of Vein-Bionic Surface Textures on the Tribological Behavior of Cylindrical Roller Thrust Bearing under Starved Lubrication. *Sci. Rep.* **2021**, *11*, 21238. [CrossRef]
171. MacLaren, A.; Kadiric, A. Elastohydrodynamic Traction and Film Thickness at High Speeds. *Tribol. Lett.* **2024**, *72*, 92. [CrossRef]
172. Maruyama, T.; Saitoh, T. Relationship between Supplied Oil Flow Rates and Oil Film Thicknesses under Starved Elastohydrodynamic Lubrication. *Lubricants* **2015**, *3*, 365–380. [CrossRef]
173. Bal, H.; Aktürk, N. Lubrication-Induced Vibrations in Rotating Shaft Systems: A Dynamic Model of Elastohydrodynamic Ball Bearings. *Proc. Inst. Mech. Eng. Part K J. Multi-Body Dyn.* **2026**, *240*, 119–136. [CrossRef]
174. Cann, P.M. Starvation and Reflow in a Grease-Lubricated Elastohydrodynamic Contact. *Tribol. Trans.* **1996**, *39*, 698–704. [CrossRef]
175. De Laurentis, N.; Kadiric, A.; Lugt, P.M.; Cann, P.M. The Influence of Bearing Grease Composition on Friction in Rolling/Sliding Concentrated Contacts. *Tribol. Int.* **2016**, *94*, 624–632. [CrossRef]
176. Zhou, Y.; Bosman, R.; Lugt, P.M. An Experimental Study on Film Thickness in a Rolling Bearing for Fresh and Mechanically Aged Lubricating Greases. *Tribol. Trans.* **2019**, *62*, 557–566. [CrossRef]
177. Bosman, R.; Lugt, P.M. The Microstructure of Calcium Sulfonate Complex Lubricating Grease and Its Change in the Presence of Water. *Tribol. Trans.* **2018**, *61*, 842–849. [CrossRef]
178. Cyriac, F.; Lugt, P.M.; Bosman, R. Impact of Water on the Rheology of Lubricating Greases. *Tribol. Trans.* **2016**, *59*, 679–689. [CrossRef]

179. Cyriac, F.; Lugt, P.M.; Bosman, R.; Venner, C.H. Impact of Water on EHL Film Thickness of Lubricating Greases in Rolling Point Contacts. *Tribol. Lett.* **2016**, *61*, 23. [CrossRef]
180. Zhou, Y.; Bosman, R.; Lugt, P.M. On the Shear Stability of Dry and Water-Contaminated Calcium Sulfonate Complex Lubricating Greases. *Tribol. Trans.* **2019**, *62*, 626–634. [CrossRef]
181. Gurt, A.; Khonsari, M.M. An Overview of Grease Water Resistance. *Lubricants* **2020**, *8*, 86. [CrossRef]
182. Ta, T.-N.; Chern, S.-Y.; Horng, J.-H.; Kuo, C.-W.; Liao, S.-J. Investigation of Performance Degradation in Calcium-Based Grease under Combined SiO2 Particle and Water Contamination. *Lubricants* **2025**, *13*, 499. [CrossRef]
183. Yang, J.; Zhang, Y.; Wang, Z.; Pu, W. Research on Mechanical Aging Behavior of Grease in Rolling Bearing. *Chin. J. Mech. Eng.* **2025**, *38*, 4. [CrossRef]
184. Atef, M.M.; Khair-Eldeen, W.; Yan, J.; Nassef, M.G.A. Investigating the Combined Effect of Multiple Dent and Bump Faults on the Vibrational Behavior of Ball Bearings. *Machines* **2022**, *10*, 1062. [CrossRef]
185. Maljaars, E.; Ravesloot, J.; Janssen, A.; Mol, H.; Murguia, C.; Fey, R. On the Potential of Rolling Bearing Strain Signals for Spall Size Estimation: Modeling and Experiments. *Mech. Syst. Signal Process.* **2025**, *240*, 113384. [CrossRef]
186. Hu, H.; Batou, A.; Ouyang, H. Friction-Induced Vibration of a Stick–Slip Oscillator with Random Field Friction Modelling. *Mech. Syst. Signal Process.* **2023**, *183*, 109572. [CrossRef]

Disclaimer/Publisher's Note: The statements, opinions and data contained in all publications are solely those of the individual author(s) and contributor(s) and not of MDPI and/or the editor(s). MDPI and/or the editor(s) disclaim responsibility for any injury to people or property resulting from any ideas, methods, instructions or products referred to in the content.